CANADIAN THESES

THÈSES CANADIENNES

NOTICE

The quality of this microfiche is heavily dependent upon the quality of the original thesis submitted for microfilming. Every effort has been made to ensure the highest quality of reproduction possible.

If pages are missing, contact the university which granted the degree.

Some pages may have indistinct print especially if the original pages were typed with a poor typewriter ribbon or if the university sent us an inferior photocopy.

Previously copyrighted materials (journal articles, published tests, etc.) are not filmed.

Reproduction in full or in part of this film is governed by the Canadian Copyright Act, R.S.C. 1970, c. C-30. Please read the authorization forms which accompany this thesis.

AVIS

La qualité de cette microfiche dépend grandement de la qualité de la thèse soumise au microfilmage. Nous avons tout fait pour assurer une qualité supérieure de reproduction.

S'il manque des pages, veuillez communiquer avec l'université qui a conféré le grade.

La qualité d'impression de certaines pages peut laisser à désirer, surtout si les pages originales ont été dactylographiées à l'aide d'un ruban usé ou si l'université nous a fait parvenir une photocopie de qualité inférieure.

Les documents qui font déjà l'objet d'un droit d'auteur (articles de revue, examens publiés, etc.) ne sont pas microfilmés.

La reproduction, même partielle, de ce microfilm est soumise à la Loi canadienne sur le droit d'auteur, SRC 1970, c. C-30. Veuillez prendre connaissance des formules d'autorisation qui accompagnent cette thèse.

THIS DISSERTATION HAS BEEN MICROFILMED EXACTLY AS RECEIVED

LA THÈSE A ÉTÉ MICROFILMÉE TELLE QUE NOUS L'AVONS REÇUE

National Library of Canada | Bibliotheque nationale du Canada

Canadian Theses Division | Division des theses canadiennes

Ottawa, Canada
K1A 0N4

0-315-26885-9

PERMISSION TO MICROFILM — AUTORISATION DE MICROFILMER

• Please print or type — Ecrire en lettres moulees ou dactylographier

Full Name of Author — Nom complet de l'auteur

AKTONO BUDHIMAN

Date of Birth — Date de naissance

15 - AUG - 1956

Country of Birth — Lieu de naissance

SURABAYA, INDONESIA

Permanent Address — Residence fixe

JALAN UNDAAN WETAN 2/29
SURABAYA, INDONESIA

Title of Thesis — Titre de la these

EXAMINATION OF FATIGUE PRECRACKING AND FRACTURE TOUGHNESS TESTING

University — Universite

UNIVERSITY OF ALBERTA

Degree for which thesis was presented — Grade pour lequel cette these fut presentee

MASTER OF SCIENCE

Year this degree conferred — Annee d'obtention de ce grade

1983

Name of Supervisor — Nom du directeur de these

DR. D.G. BELLOW, AND DR. D.R. BUDNEY

Permission is hereby granted to the NATIONAL LIBRARY OF CANADA to microfilm this thesis and to lend or sell copies of the film.

The author reserves other publication rights, and neither the thesis nor extensive extracts from it may be printed or otherwise reproduced without the author's written permission.

L'autorisation est, par la présente, accordée à la BIBLIOTHÈQUE NATIONALE DU CANADA de microfilmer cette thèse et de prêter ou de vendre des exemplaires du film.

L'auteur se réserve les autres droits de publication; ni la thèse ni de longs extraits de celle-ci ne doivent être imprimés ou autrement reproduits sans l'autorisation écrite de l'auteur.

Date

JUNE 30th - 1983

Signature

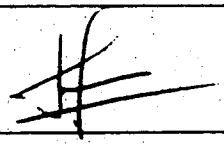

NL-91 (4/77)

THE UNIVERSITY OF ALBERTA

Examination of Fatigue Precracking and Fracture Toughness Testing

by

© Artono Budhiman

A THESIS

SUBMITTED TO THE FACULTY OF GRADUATE STUDIES AND RESEARCH

IN PARTIAL FULFILMENT OF THE REQUIREMENTS FOR THE DEGREE

OF Master of Science

Department of Mechanical Engineering

Edmonton, Alberta

Fall 1983

THE UNIVERSITY OF ALBERTA

RELEASE FORM

NAME OF AUTHOR Artono Budhiman

TITLE OF THESIS Examination of Fatigue Precracking and Fracture Toughness Testing

DEGREE FOR WHICH THESIS WAS PRESENTED Master of Science

YEAR THIS DEGREE GRANTED Fall 1983

Permission is hereby granted to THE UNIVERSITY OF ALBERTA LIBRARY to reproduce single copies of this thesis and to lend or sell such copies for private, scholarly or scientific research purposes only.

The author reserves other publication rights, and neither the thesis nor extensive extracts from it may be printed or otherwise reproduced without the author's written permission.

(SIGNED) .....

PERMANENT ADDRESS:

Jalan Undaan Wetan 2/29

Surabaya

Indonesia

DATED May-16-1983

THE UNIVERSITY OF ALBERTA

FACULTY OF GRADUATE STUDIES AND RESEARCH

The undersigned certify that they have read, and recommend to the Faculty of Graduate Studies and Research, for acceptance, a thesis entitled Examination of Fatigue Precracking and Fracture Toughness Testing submitted by Artono Budhiman in partial fulfilment of the requirements for the degree of Master of Science.

Supervisors

Date May-16-1983

Abstract

The purpose of this investigation was to examine the restrictions given by standards on the use of maximum stress intensity factor (Kfmax) and the stress ratio (R) during fatigue precracking for the preparation of a fracture specimen. The relevant standards are ASTM E-399:81 and BS 5447:77 for plane strain fracture toughness (K1c), and BS 5762:79 for the Crack Opening Displacement (δ). The standards restrict Kfmax to avoid overestimation of toughness values resulting from large monotonic plastic zone size. The R-ratio is restricted to 0.1 or lower, although the standards do not explain a reason for the restriction. Experimental results confirmed that this restriction maximizes crack propagation rate, a probable reason for the R restriction.

By investigating the effect of Kfmax and R on Kq (provisional K1c value) and δm (δ maximum) it was revealed that overestimation of Kq and δm could be associated with crack blunting as a result of either a large monotonic plastic zone size (r_y) or a large reverse plastic zone size (r_{yo}). It is widely accepted that high Kfmax creates large r_y where high stress intensity range (ΔK) creates large r_{yo}. The results show that restricting R introduces an unnecessary constraint and maximizes the reverse plastic zone size, thus possibly resulting in blunting of the crack.

For the material used in this experiment (AISI 4140 σ_y=797MPa σ_m=962MPa) the fracture test results show that in

order that the lower limit for Kq (=67MPa$\sqrt{m}$) be evaluated, Kfmax should be restricted to less than 0.42Kq. Similarly for evaluation of lower values of δm (=0.025mm), Kfmax should have a value less than $0.38\sigma_y\sqrt{B}$. The ASTM E-399 requires Kfmax≤0.6Kq, the BS 5447 requires Kfmax≤0.7Kq and the BS 5762 requires Kfmax≤$0.63\sigma_y\sqrt{B}$, and hence none are sufficiently stringent to correctly evaluate the toughness value of the material used.

Based on test results of specimens fatigue precracked at different R-ratios it is apparent that higher R could produce a sharper fatigue crack. This therefore suggests that the R restriction is an unnecessary constraint, and perhaps should be given further consideration.

Acoustic emission was monitored throughout the period of fatigue precracking. The purpose was to compare the amount of plastic deformation at the crack tip which was related to degree of crack blunting. The result showed that monitoring acoustic emission gives a method of warning for any possible damage on the fatigue crack during the fatigue precracking process.

Acknowlegement

The author wishes to extend his sincere appreciation to Dr D.G. Bellow and Dr D.R. Budney for supervising this thesis, he is grateful to Dr F.H. Vitovec for advice received.

He would also like to thank the Mechanical Engineering Department of the University of Alberta for providing the financial assistance which made his study possible.

Table of Contents

Chapter		Page
1.	Introduction	1
2.	General Description of Fracture Mechanics Design Concept	4
	2.1 Introduction	4
	2.2 Material Toughness	5
	2.3 Effects of Crack tip Plastic Zone	10
	2.4 Experimental Evaluation of Material Toughness	13
	2.4.1 Plane Strain Fracture Toughness	13
	2.4.2 Plane Stress Fracture Toughness	14
3.	Standard Technique for Material Toughness Evaluation	18
	3.1 Introduction	18
	3.2 Specimen Preparation for K1c and COD Testing	20
	3.2.1 K1c Standards (ASTM E-399:81; BS 5447:77)	20
	3.2.2 COD Standard (BS 5762:79)	22
	3.3 Fracture Test	23
	3.3.1 K1c Fracture Test (ASTM-E399; BS 5447)	23
	3.3.2 COD Fracture Test	25
	3.4 Effect of Kfmax on K1c and COD	26
	3.4.1 Effects of Kfmax on the K1c	26
	3.4.2 Effect of Kfmax on the COD	32
	3.5 Effect of R-ratio on the K1c and COD	33
4.	Acoustic Emission Detection	35
	4.1 Introduction	35
	4.2 Acoustic Emission Monitoring of Fatigue Crack Growth	39

4.3 Acoustic Emission Monitoring of Crack Growth and Fracture in Quasi-static Loading 42

5. Experimental Procedure 43

5.1 Introduction 43

5.2 Test Material 43

5.3 Specimen Preparation 45

5.4 Fatigue Precracking 46

5.5 Acoustic Emission Detection 47

5.6 Crack Length Measurement 49

5.7 Data Acquisition 50

5.8 Fracture Toughness Testing 51

6. Experimental Results and Discussion 52

6.1 Fatigue Precracking 52

6.2 Fracture Test 63

7. Conclusions 76

Bibliography 79

APPENDIX 1 - Crack Propagation Measurement 84

APPENDIX 2 - Preloading of Specimen for Acoustic Emission Test 89

APPENDIX 3 - Data Acquisition 91

List of Tables

Table		Page
1	Indication of cyclic softening by the ratio of the material ultimate to yield stress	30
2	Rolling direction mechanical properties of AISI 4140 steel	44
3	Chemical analysis of AISI 4140 steel	44
4	Kq and CODm values obtained for different Kfmax and R-ratio	74-75

List of Figures

Figure		Page
1	Mode of fracture ; (a)opening, (b)shearing, (c)tearing	5
2	Three dimensional crack tip and stress system	6
3	Three-point bend specimen	8
4	Effect of thickness on fracture toughness	9
5	Effect of temperature and loading speed on fracture toughness	9
6	Fracture mechanics design curve	11
7	Variation of crack tip plastic zone through the thickness of plate	12
8	Plastic hinge	17
9	Typical load versus clip-gauge displacement curves for K1c test	25
10	Typical load versus clip-gauge displacement curves for COD test	27
11	Effect of Kfmax on Kq (typical experimental results)	28
12	Acoustic emission waveform detected by transducers; (a)burst emission, (b)continuous emission	36
13	Parameter for characterizing an acoustic emission event	36
14	Schematic representation of components in energy measuring device (ref: Harris and Bell, 1977)	38
15	Three-point bending specimen design	45
16	Experimental set-up for monitoring fatigue precracking parameters	48
17	Crack length measurement and acoustic emission monitoring fracture specimen under three-point fatigue loading	49

Figure Page

18 Number of fatigue cycles required to reach 0.5W crack lentgh as a function of Kfmax and R.....53

19 Number of fatigue cycles required to reach 0.5W crack length as a funtion of ΔK.....54

20 The crack propagation rate of AISI 4140 (specimen C0, σ_y=780 MPa).....56

21 Monitored value of R-ratio and Kfmax during the fatigue precracking.....57

22 Monitored value of total emission and crack length during the fatigue precracking.....58

23 Number of acoustic emission counts per-cycle for differing Kfmax and R-ratio.....60

24 Typical load also total emission versus clip-gauge displacement of the fracture test; (a)No pop-in, (b)Pop-in occurred.....61-62

25 Effect of Kfmax on Kq at (a)R=0.1, (b)R=0.3, (c)R=0.5 and (d)R=0.1 - 0.5.....64-67

26 Effect of Kfmax on CODm at (a)R=0.1, (b)R=0.3, (c)R=0.5 and (d)R=0.1 - 0.5.....69-72

I Relationship of crack length to clip-gauge displacement.....84

II Load versus displacement curves for different crack length of three-point bend specimen.85

III Measurement of crack length using crack-gauge TK-09-CPA01-005/S, Inter Technology Limited.....87

IV Comparison of crack length measurement using (a)crack gauge and (b)clip-gauge.....88

V Preloading fixture (ref: Dunegan et al, 1968).....89

VI Photo-elastic stress pattern of single-edge-notch fracture toughness specimen: (a)Preloaded as suggested by Dunegan et al, 1968 (b)Loaded in tension (c)Overall view of the specimen loaded in tension...90

Figure Page

VII Block diagram for data acquisition system for fatigue precracking of fracture specimens.....93

Nomenclature

B	Specimen thickness.
COD (δ)	Crack Opening Displacement as defined by BS 5762:1979.
D	Distance measured from an acoustic emission source.
E	Modulus of elasticity.
J	A path independent integral as a measure of material toughness.
J1c	Critical value of J (ASTM E-813:1981).
K	Stress intensity factor. (Ksi√in ; Mpa√m)
Kc	Plane stress fracture toughness.
K1, K2, K3	Stress intensity factor at mode I, II, III.
K1c	Plane strain fracture toughness (ASTM E-399:1981 ; BS 5447:1977).
K1d	Dynamic fracture toughness.
Kf	Stress intensity factor during fatigue precracking.
Kfmax	Maximum fatigue stress intensity factor.
Kq	Provisional value of K1c.
Kql	Lower limit of Kq results from a 'perfectly' prepared fatigue crack.
ΔK	Stress intensity range (Kfmax - Kfmin).
N	Number of acoustic events.
Nr	Number of ring down counts.
Pmax	Maximum applied load.

Pq	Load corresponds to Kq.
P_5	Load corresponds to 5% offset in K1c method.
R	Stress ratio (Kfmin/Kfmax or Pmin/Pmax).
R-curve	Resistance curve, a measure of plane stress fracture toughness as defined by ASTM E-561:1981.
V	Clip gauge displacement.
Vi, Vc	Clip gauge displacement at initiation and critical crack growth.
Vm, Vu	Clip gauge displacement at maximum and unstable crack growth.
W	Specimen width.
Y	Compliance function as defined by BS 5762:1979.
Z	Extension length for clip gauge mount.
a, ac	Crack length and critical crack length.
c	A constant.
da/dn	Crack propagation rate.
dN/dn	Number of acoustic events per fatigue cycle.
dNr/dn	Number of acoustic ring down counts per fatigue cycle.
$f_{ij}(\theta)$	A function defining a structure of certain geometry containing a crack at a certain orientation.
m	A constant.
p	Coefficient of plastic hinge.
r, θ	Polar coordinate.

r_y	Irwin plastic zone size (for both plane strain and plane stress).
r_{y1}, r_{y2}	Plastic zone size at fatigue precracking and fracture test.
r_{yo}	Reversed plastic zone size.
α	Proportionality value defined as Kfmax/Kql.
α_1	Proportionality value defined as Kfmax/(σ_y/B).
δc, δi	Critical and initiation Crack Opening Displacement.
δu, δm	Unstable and maximum Crack Opening Displacement.
ϵ_y	2% yield strain.
λ	Experimentally determined constant for COD measurement.
σ_d	Design stress.
σ_m	Ultimate stress.
σ_y	Yield stress (2% proof stress).
σ_{y1}, σ_{y2}	Yield stress at temperature of fatigue precracking and fracture test respectively.

1. Introduction

The increased complexity of modern structures, the use of high strength materials, thick sections, welded joints and the severity of the service environment conditions has increased the need for incorporating fracture mechanics in design. Knowledge of fracture mechanics enables designers to specify the toughness value of a material so that under the conditions of service, the designed structure will not fail in the fracture mode.

Material toughness can be described in terms of the critical stress intensity factor under conditions of plane stress (Kc) or plane strain (K1c) for slow loading and linear elastic behaviour. For elastic-plastic behaviour the material toughness is measured in terms of parameters such as R-curve, 'J integral (J1c) and Crack Opening Displacement (COD).

Standard techniques for K1c (ASTM E-399, BS 5447) and COD (BS 5762) measurement give guidelines and restrictions for preparation of test piece specimens. During fatigue precracking of the specimen, the standards place a restriction on the maximum stress intensity factor (Kfmax) derived from the maximum cyclic load level. In the standards for K1c testing, this restriction is expressed as

$$Kfmax \leq \alpha(\sigma_{y,1}/\sigma_{y,2})Kq,$$

where Kq is the provisional value of K1c. The yield stress

ratio σ_{y1}/σ_{y2} is equal to one if the specimen is prepared and fractured at the same environmental temperature. The value of α is a ratio of crack tip plastic zone size during fatigue precracking to plastic zone size at fracture. Based on experiments by Brown and Srawley (1970), the American Society for Testing and Materials (ASTM) E-399:1981 Standard for K1c stipulates that α=0.6 should be used. The British Standard BS 5447:1977 for K1c has a more relaxed value of α=0.7 as a restriction. The value was based on experiments by May (1970).

The restriction for Kfmax was placed to avoid a possible over-estimation of K1c value as a result of a large plastic zone size ahead of the crack tip formed during fatigue precracking with a high Kfmax.

In the British Standard BS 5762:1979 for COD testing, the Kfmax restriction is expressed as

$$Kfmax \leq \alpha_1 \sigma_y \sqrt{B} ,$$

where σ_y is the yield stress and B is the thickness of the specimen. The restriction is derived on the basis of assurance that the state of stress at the crack tip will remain plane during fatigue precracking of the specimen. The value of α_1=0.63 was experimentally determined.

These values for α and α_1 have often been considered to be too small for some materials such as 2014-T6 aluminum (Kaufman,1977) and too high for others such as 3Ni,1Cr,0.5Mo

(Clark, 1979).

A further restriction for all three standards is that the stress ratio (R) during fatigue precracking should be between 0 and 0.1 for BS:5447 and BS:5762 and should be between -1 and 0.1 for ASTM E-399. This R-ratio restriction maximizes the crack initiation and propagation speed.

With a constant Kfmax, a higher value of R-ratio would be expected to produce a smaller crack tip reversed plastic zone size hence a sharper crack tip. This would then be closer to the simulated ideal plane crack that is assumed in the theoretical derivation of the stress intensity factor K. If this is so, limiting $R \leq 0.1$ may lead to over-estimation of fracture toughness.

In this report, two sets of tests were done to investigate the effect of high Kfmax on Kq and COD, and the effect of high R-ratio on Kq and COD. During fatigue precracking in the preparation of the toughness specimen, acoustic emission was continuously monitored so that the history of the crack tip plastic zone development could later be related to the subsequent toughness value Kq and/or COD. High Kfmax as well as low R-ratio values were expected to create a larger plastic zone hence greater accumulated acoustic emission counts. If this is the case, a continuous monitoring of the acoustic emission during fatigue precracking of the specimen may be useful in estimating an allowable Kfmax value and a more sensible R-ratio value.

2. General Description of Fracture Mechanics Design Concept

2.1 Introduction

Mechanical failure can be identified by its general categories, some common modes being: failure by elastic instability (buckling), failure by excessively large elastic deformation (jamming), failure by gross plastic deformation (yielding), failure by tensile instability (necking), failure by environmental corrosion, failure by fatigue and failure by fast fracture (cracking).

Technological advances permitting increased working stresses and reduced safety factors have been achieved due to advancements in stress analysis techniques and the use of higher strength materials. However, the application of thicker sections, joining of components by welding, cyclic loads and severe environmental conditions reduce the capacity of materials to absorb local plastic strain without fracture.

Fracture mechanics design concepts have been developed for failure by brittle fracture. The design concepts provide design engineers quantitative guidelines relating material toughness to the critical defect size and the design stress.

Because of the existence of advanced stress analysis techniques including numerical methods, the stress levels in complex structures can now be determined. Some defects existing in structures can be detected using ultrasonic methods. The fracture mechanics concept uses information on

stress levels and crack size or possible crack size during the service life time of a structure, for the prediction of unstable crack growth. Provided that material toughness can be evaluated accurately, the problem of failure due to fracture can be minimized by design.

2.2 Material Toughness

Linear elastic fracture mechanics provides an analytical procedure that relates the stress magnitude in the vicinity of a crack tip to the nominal applied stress, size, shape, and orientation of the crack-like discontinuity. The procedure has been established by first defining the three modes of relative displacement of two crack surfaces, namely the opening, shearing and tearing modes (Fig.1 a,b,c). These displacement modes represent the local deformation in an infinitesimal element containing a crack front. In any problem the deformation at the crack tip can be treated as one or a combination of these local displacement modes.

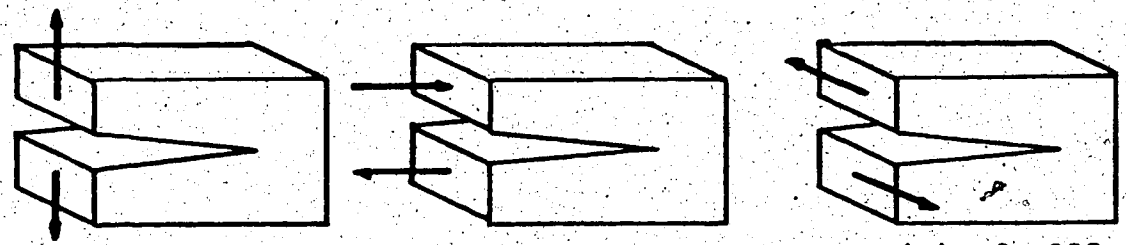

Figure 1 Mode of fracture ; (a)opening, (b)shearing, (c)tearing

By using a method that was developed by Westergaard (1939), Irwin (1957) found that the stress and displacement fields (Fig.2) in the vicinity of the crack tip subjected to the first mode of deformation (at plane strain) are given by ,

$$\sigma_{11} = (K1/\sqrt{2\pi r})\ \cos(\theta/2)\ [\ 1 - \sin(\theta/2)\ \sin(3\theta/2)]$$
$$\sigma_{22} = (K1/\sqrt{2\pi r})\ \cos(\theta/2)\ [\ 1 + \sin(\theta/2)\ \sin(3\theta/2)]$$
$$\sigma_{12} = (K1/\sqrt{2\pi r})\ \sin(\theta/2)\ \cos(\theta/2)\ \cos(3\theta/2)$$
$$\sigma_{33} = \nu(\sigma_{11} + \sigma_{22})\ ;\ \sigma_{13} = \sigma_{23} = 0 \qquad (1)$$
$$u_1 = (K1/G)(r/2\pi)^{1/2}\cos(\theta/2)\ [\ 1 - 2\nu + \sin^2(\theta/2)]$$
$$u_2 = (K1/G)(r/2\pi)^{1/2}\cos(\theta/2)\ [\ 2 - 2\nu - \cos^2(\theta/2)]$$
$$u_3 = 0$$

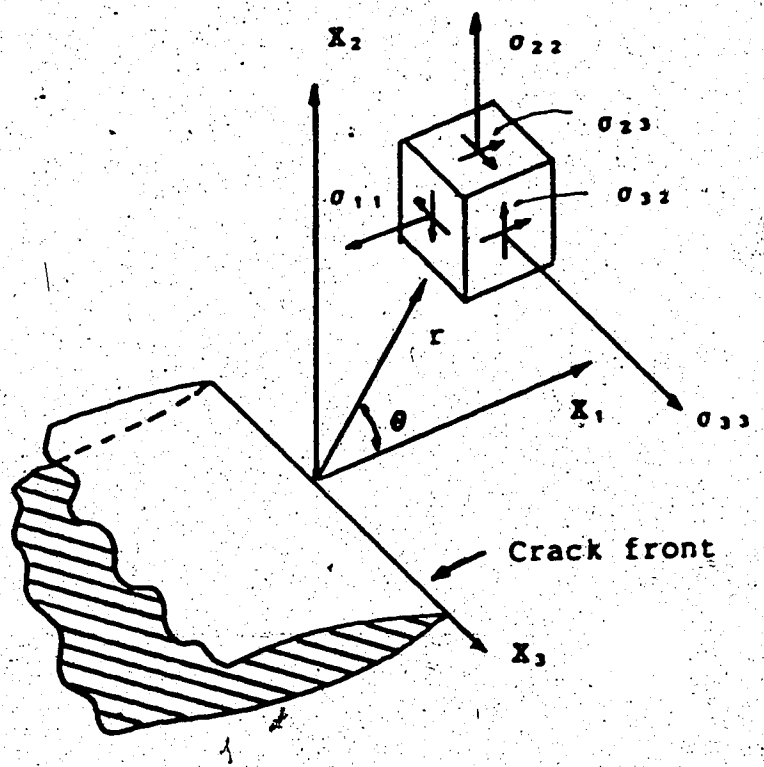

Figure 2 Three dimensional crack-tip and stress system

G is the shear modulus of elasticity.

The stresses in tensorial form are

$$\sigma_{ij}=(K_m/\sqrt{2\pi r})f_{ij}(\theta) \qquad (2)$$

K_m is the stress intensity factor of mode m=1,2,3; $f_{ij}(\theta)$ is a geometrical function. To convert the above expression for plane stress, set $\sigma_{33}=0$ and replace υ by $\upsilon/(1+\upsilon)$. Equation (2) can be rewritten as

$$K_m=(\sigma_{ij}\sqrt{2\pi r})/f_{ij}(\theta) \qquad (3)$$

(note that summation convention is suppressed).

For plate containing a through thickness crack of length 2a, the function $f_{ij}(\theta)$ is unity and 2r is replaced by a

$$\begin{aligned} K1&=\sigma_{11}\sqrt{\pi a} \\ K2&=\sigma_{12}\sqrt{\pi a} \\ K3&=\sigma_{23}\sqrt{\pi a} \end{aligned} \qquad (4)$$

The function $f_{ij}(\theta)$ for different geometry and crack orientation are commonly available in textbooks. For a useful example, the stress intensity factor of a center notch three point loading fracture specimen is expressed in Eqn. 5 (ASTM E-399:81) as shown in Fig.3.

At a slow loading rate, as the crack length approaches a critical value of ac, a critical value of K will be reached and followed by onset of an unstable crack growth.

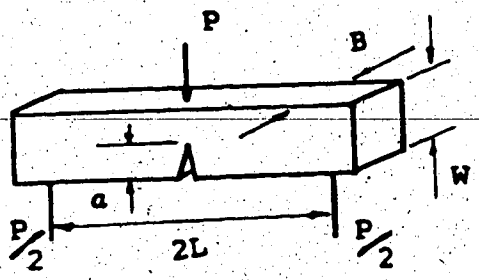

$$K = (3PL/BW^{3/2}) \left[1.93 (a/W)^{1/2} - 3.07 (a/W)^{3/2} + \ldots \right] \quad (5)$$

Figure 3 Three-point bend specimen

This critical value of K is also known as the material toughness and is designated Kc. Its value depends on the material, state of stress, temperature and loading speed. It is known that Kc decreases with an increase in thickness (Fig.4), reaching a rather constant minimum value K1c when mode I plane strain conditions are satisfied. Knowledge of K1c therefore provides a conservative approach to the fracture problem.

Experiments have shown that for the same material both Kc and K1c value reduce as the temperature decreases (Fig.5). For impact loading the K1c value reduces to become K1d (K1d is the plane strain dynamic fracture toughness).

Experimental techniques exist for evaluation of toughness values Kc and K1c, and are discussed in a later chapter. The fracture design curves are normally presented

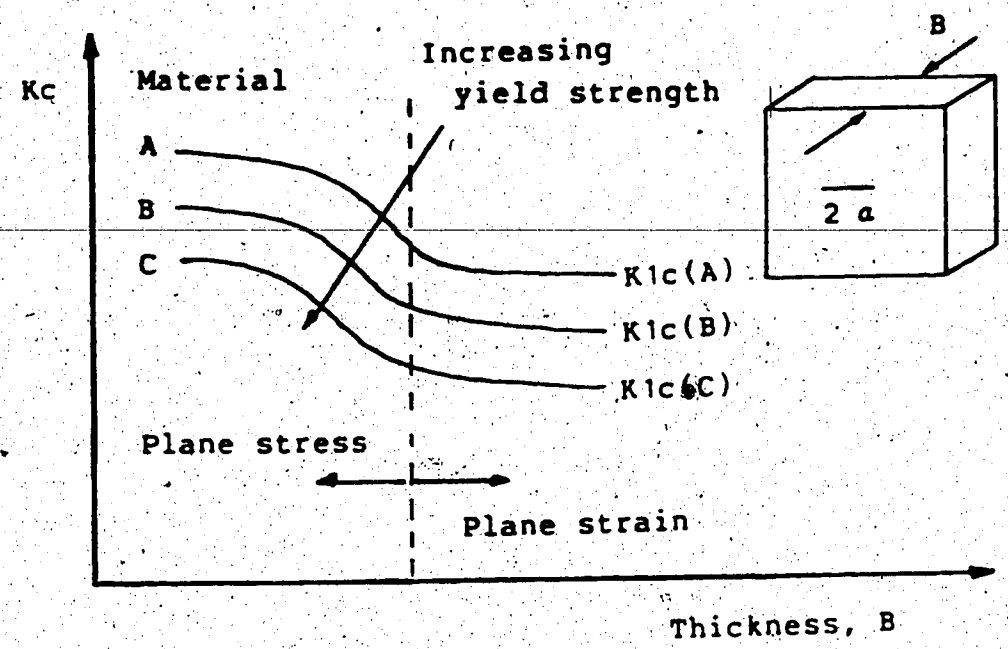

Figure 4 Effect of thickness on fracture toughness

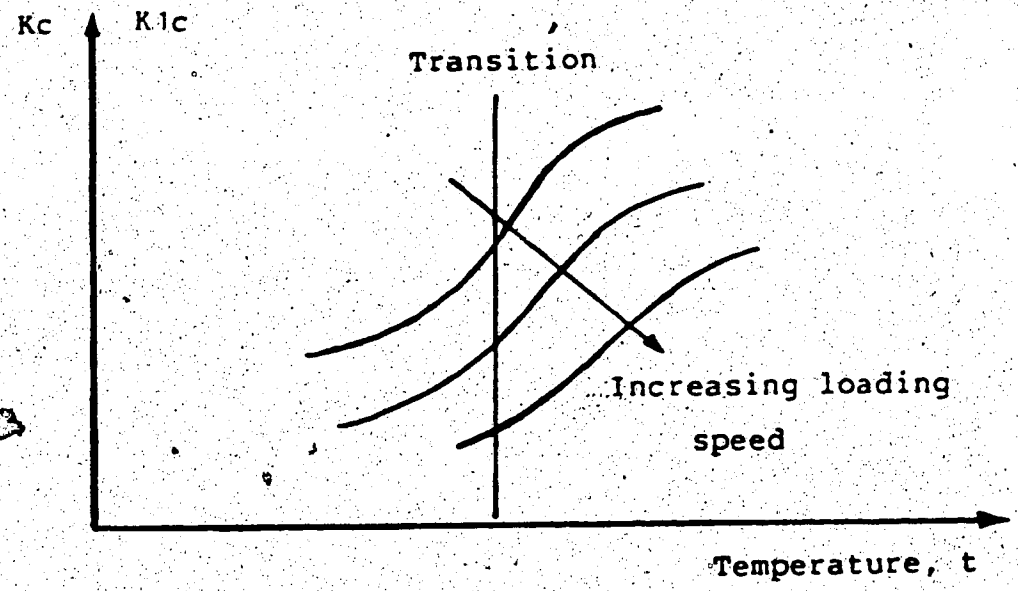

Figure 5 Effect of temperature and loading speed on fracture toughness

as shown in Fig.6. At a design stress σ_d a defect size of a_c would be critical for the material C but considerably safer when material B is used. In general the value of Kc is about 2 to 10 times larger than K1c. The reason has been related to the large plastic zone at the vicinity of the crack tip. As a result of this plasticity, the linear elastic fracture mechanics does not apply and alternative approaches have been considered namely the R-curve , Crack Opening Displacement (COD) or J integral methods. In general these approaches are known as elastic-plastic fracture mechanics.

2.3 Effects of Crack tip Plastic Zone

Linear elastic fracture mechanics explicitly assumes that the material behaves in a purely elastic manner. In particular the stress field equations described in Eqn.1 show that the stress magnitude approaches infinity as the r (of the r,θ coordinate) approaches the crack tip. In practice most materials deform plastically once the yield stress is reached. This region of plastic deformation is known as the plastic zone as illustrated in Fig.7. Irwin (1957) has suggested that the size of plastic zone r_y should be

$$r_y = 1/2\pi(K/\sigma_y)^2 \quad \text{for plane stress,}$$
$$r_y = 1/6\pi(K/\sigma_y)^2 \quad \text{for plane strain.} \qquad (6)$$

Note that the plane stress plastic zone size (r_y) is three

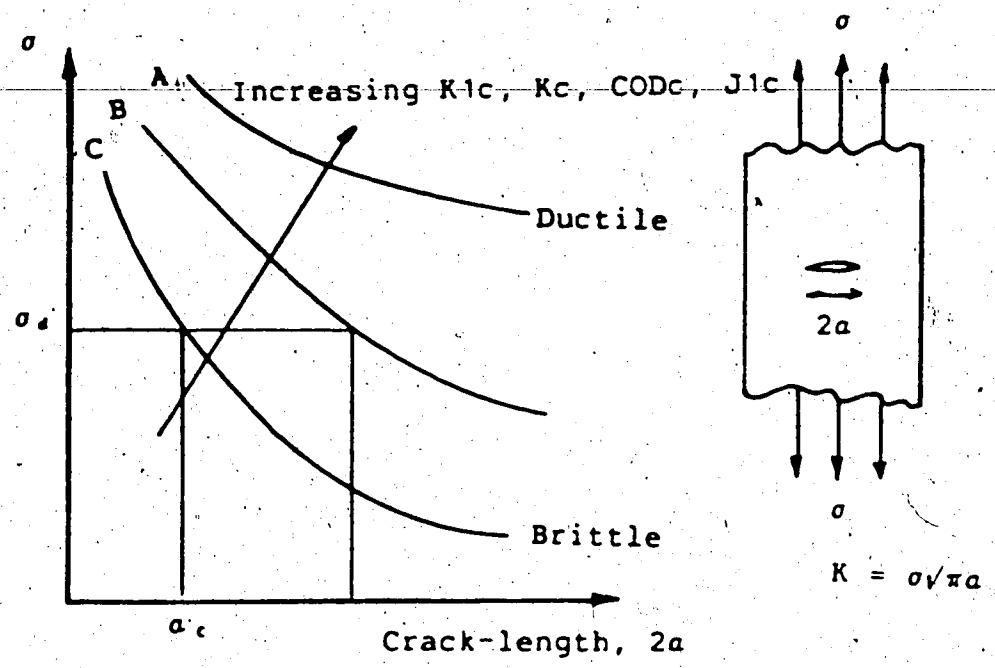

Figure 6 Fracture mechanics design curve

times bigger than the plane strain value and is also inversely proportional to the square of the yield stress σ_y. This often explains the difficulties encountered when fracture toughness for material with low yield stress is to be evaluated.

The existence of the plastic zone in reality makes the evaluation of K1c difficult. In theory the plane strain fracture toughness evaluation does not allow for any plasticity at the crack tip. In practice this could be approximated by making the test specimen dimensions large enough so that the plastic zone size is small in comparison.

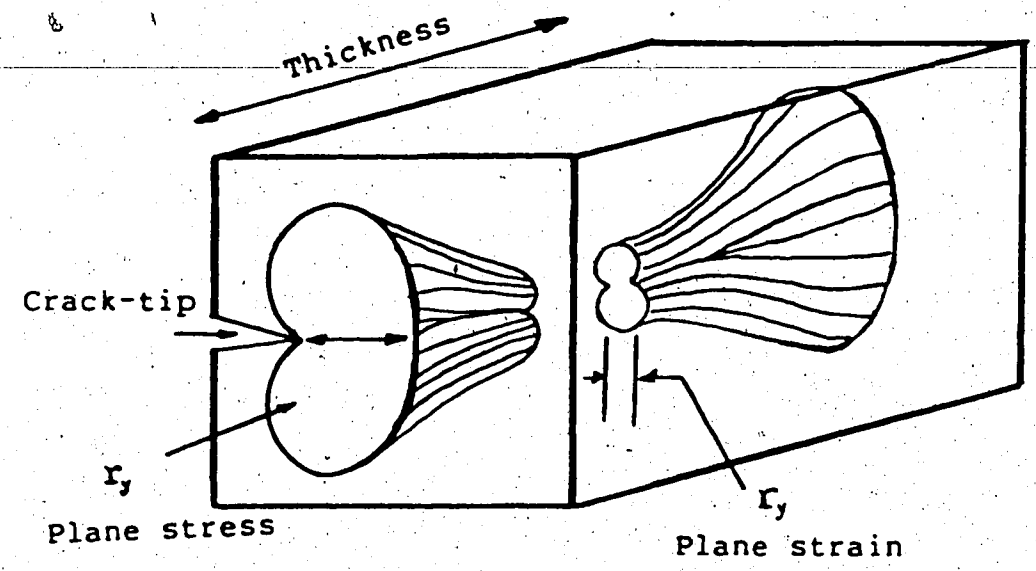

Figure 7 Variation of crack-tip plastic zone through the thickness of plate

Smallest specimen dimension of approximately 50 times the estimated plastic zone size is normally considered adequate to approximate linear elastic behaviour near the crack tip. The value of '50' is normally adopted as a guideline for estimating the test specimen dimensions in evaluating K1c.

In the design of aircraft and pressure vessels the plane stress problem is of great practical importance. Plate materials are commonly used and toughness values of available thicknesses are evaluated. Unfortunately the plane stress plastic zone size is large and often results in inadequate specimen dimensions for the K1c test.

2.4 Experimental Evaluation of Material Toughness

2.4.1 Plane Strain Fracture Toughness

Plane strain fracture toughness K1c is evaluated experimentally. Provided the estimated plastic zone size is small in comparison to the specimen dimensions, linear elastic fracture mechanics can be approximated. An ideal specimen should have a geometry that is easily prepared and posseses geometry that permits Eqn.1 to be valid. The specimen should have a crack with a sharp tip that would approximate the ideal plane crack assumed in the analytical stress field representation (Eqn.1).

Although a machined notch may not resemble the ideal plane crack presented in the analysis, a fatigue precrack can be developed as an extension of this machined notch. If this fatigue precrack is prepared carefully, the ideal plane crack can be closely simulated.

When all proper specimen preparations are made, the fracture test is done simply by loading slowly. The load at which an unstable crack growth starts is called the fracture load Pc and when applied to the Eqn.5, the fracture toughness K1c is obtained.

Standard procedures for the K1c test are now available to ensure repeatable test results. The ASTM E-399:81 and the British Standard BS 5447:1977 are the accepted standards for evaluating K1c.

2.4.2 Plane Stress Fracture Toughness

Linear elastic fracture mechanics does not apply when large plastic deformation at the crack tip occurs. The general concept however could be extended to produce an alternative method called R-curve. The method makes the evaluation of plane stress toughness Kc possible (ASTM E-561:1981). However, the specimen size for R-curve evaluation is so large that it often becomes impractical.

Rice (1968) introduced a new approach to the fracture problem by defining a path independent integral energy method. The method is known as the J integral method. Since it is based on an independent path analysis, the effect of the large plastic zone is avoided if a path taken outside this plastic zone is used in the calculation. Indeed the method is claimed to represent toughness values from plane strain to plane stress conditions. To date a working standard has been introduced for plane strain conditions only (ASTM E-813:1981). The standard permits evaluation of the critical value J1c which could be related to the plane strain fracture toughness K1c as

$$J1c=(1-\upsilon^2)K1c^2/E \qquad (7)$$

Lately a single specimen J integral has been in the forefront of the J integral technique, the method requires very accurate instrumentation and a computer for calculation of unloading compliance. The standard for J integral

evaluation requires multiple specimens, therefore within the linear elastic region (J1c), the J integral method has no obvious advantage over the linear elastic fracture mechanics approach.

In 1961, Wells introduced the Crack Opening Displacement method. Assuming plasticity at the crack tip, the strip yield model by Dugdale (1960) can be used to relate the COD to the applied stress and crack length. The basic relationship was further developed by Burdekin and Stone (1966) and expressed as

$$\delta=(8\sigma_y a/\pi E)\{\ln \sec(\pi\sigma/2\sigma_y)\} \tag{8}$$

where δ is the Crack Opening Displacement according to Wells. A reasonable approximation for the above equation would be

$$\delta=\pi a\sigma^2/E\sigma_y \tag{9}$$

provided σ/σ_y is small (ie: in the linear region). When a large area of crack tip plasticity is considered, the equation is expressed as

$$\delta=K^2(1-\upsilon^2)/\lambda E\sigma_y \tag{10}$$

The values of λ which have been reported in the literature depend upon the exact location of the crack tip in their

evaluation. The British Standard BS 5762:1979 for COD gives this value of $\lambda = 2$. Usually, COD measurement is made on three point bend specimens of similar type as the K1c specimen. Experimental evaluation is as follows: since the whole uncracked ligament is above yield, it may be considered a plastic hinge (Fig.8) with the centre of rotation at a distance $p(W-a)$ from the crack tip. The crack edges are assumed to remain straight. The rotational factor p has to be determined experimentally. A similar triangle for clip-gauge displacement (V) and COD can be constructed and an expression derived from it is

$$V/\{a+p(W-a)\} = \delta/p(W-a)$$

or

$$\delta = \{p(W-a)V\}/\{a+p(W-a)\} \qquad (11)$$

Experiment has shown that the value of p varies from 0.08 to 0.4 for COD of 0.0004 to 0.012 inches (0.01 to 0.3 mm) (Robinson and Tetelman, 1973). The BS 5762 has adopted p of 0.4 . As can be seen from Eqn.9, δ is analogous to the K1c when the critical value δc is reached. The K1c and COD (δc) can be related as

$$\delta c/\epsilon_y = (K1c/\sigma_y)^2 \qquad (12)$$

Since the method was developed on the basis of crack tip plasticity, it can be used to evaluate fracture toughness of

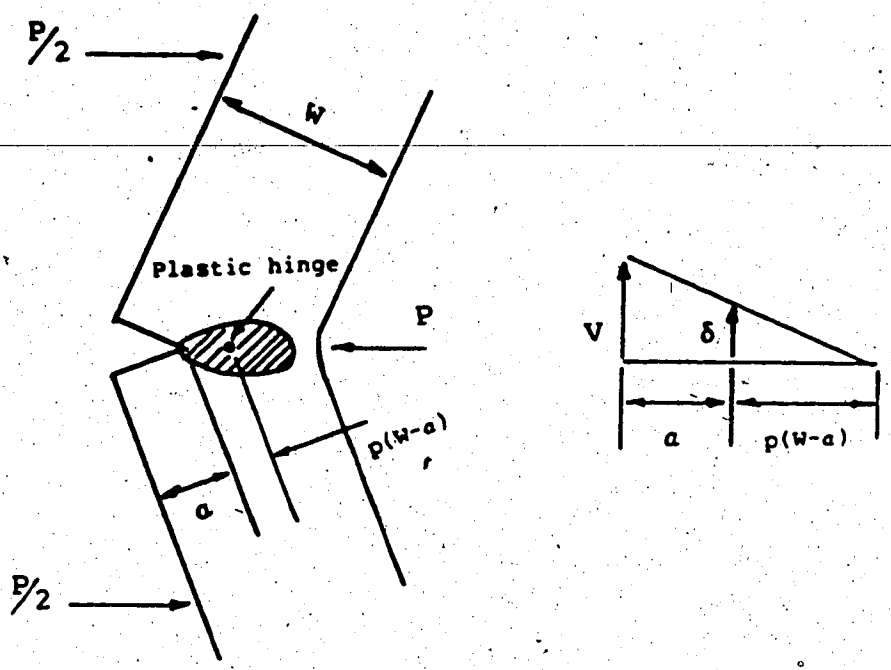

Figure 8 Plastic hinge

linear elastic, elastic-plastic and plastic behaviour. For a linear elastic condition, the COD method has no real advantage over the K1c method. There are many practical materials for which the K1c value can not be obtained. For this case the COD method becomes useful. The present standard for the COD fracture toughness measurement is given by the British Standard BS 5762:1979. Most of the specimen preparation procedures have been taken from the plane strain fracture toughness K1c standard (BS 5447). For the COD method, tests can be carried out on specimens of the full thickness available.

3. Standard Technique for Material Toughness Evaluation

3.1 Introduction

There are presently five standard techniques available for evaluation of material toughness under quasi-static loading. These are ASTM E-399:1981 for K1c, BS 5447:1977 for K1c, BS 5762:1979 for COD, ASTM E-561:1981 for R-curve, ASTM E-813:1981 for J1c. Each of these standards has its own advantages as well as disadvantages. Toughness values from any standard are subject to error, some of which may be due to lack of technical expertise.

The standards for R-curve and J1c are new. Although their concept appears to be very promising, the lack of service experience for these techniques limit their present usefulness to the design engineer. The standards for K1c and COD, on the other hand have acquired wide acceptance. Material toughness expressed in terms of K1c for linear elastic behaviour and COD for elastic plastic behaviour are used in many fracture mechanics design practice.

The K1c and COD test involve the following two stages:

a)the development by fatigue loading of a crack from a machined notch in a test piece (specimen preparation); b)the propagation of that crack by applying an increasing force which may cause bending or tension to produce a fracture (fracture test).

The K1c standards utilize two[1] types of test piece namely the compact test specimen (tensile test) and the three point bend specimen, while the COD standard employs only the bend test.

Although it has now been established that reproducible K1c values could be obtained for the same material by different laboratories within about 15%, there are still unsettled difficulties in following the restrictions contained in the Standard (Towers, 1981). Specifically, these problems are the estimation of an allowable maximum stress intensity factor Kfmax and the stress ratio R during fatigue precracking. The guideline for specimen preparation limits the Kfmax in order that the monotonic plastic zone size during this time is less than the plastic zone size during the fracture test. A high Kfmax value results in an over-estimated K1c value. Without explanation the Standards also restrict the fatigue precracking stress ratio R to be between 0 and 0.1 for BS 5447 and between -1 and 0.1 for ASTM E-399. A study related to these restrictions is presented in Sections 3.4 and 3.5 of this thesis.

The COD Standard is intended to give fracture toughness evaluation for elastic-plastic to fully plastic fracture behaviour in which the K1c technique is not valid. The COD Standard limits the fatigue precracking stress level differently than does the K1c Standards. This restriction ensures that the plane strain plastic zone size (r_y) is less

[1] ASTM E-399:81 has four types of test piece.

than one fiftieth of the specimen width B during fatigue precracking. The COD Standard adopted the R restriction given by the K1c Standard BS 5447.

3.2 Specimen Preparation for K1c and COD Testing

3.2.1 K1c Standards (ASTM E-399:81; BS 5447:77)

The derivation of linear elastic fracture mechanics relates the stress intensity factor K to the stress level and crack size present in any structural geometry and crack orientation (Eqn.1). The analysis is based on an assumption of the existence of an ideal plane crack and the stress is at a state of plane strain (mode I). Experimental evaluation of material toughness based on linear elastic fracture mechanics (K1c) requires preparation of the specimen to simulate these ideal conditions. For a valid K1c evaluation, it is necessary that the smallest specimen dimension be of an order 50 times greater than the plane strain plastic zone size. This restriction which is adopted in both ASTM E-399:1981 and BS 5447:1977, is expressed as

$$a,\ B \text{ and } W/2 \geq 2.5(K1c/\sigma_y)^2 \qquad (13)$$

where a, B, W/2 are the crack length, thickness and half width of the test piece. It is noted that even before a K1c test specimen can be machined, the K1c value to be obtained must already be known or at least estimated. For this reason

both standards provide a limited guideline for estimating specimen dimensions by the ratio of yield strength to modulus of elasticity, σ_y/E.

It has been evident that the fatigue precracking process must be closely controlled in order to avoid damage and the development of an unsatisfactory fatigue precrack. The procedure ensures that the last 2.5% of the overall length of the notch plus fatigue precrack is loaded at a maximum stress intensity level during fatigue (Kfmax) such that the Kfmax value is less than the Kq value determined in the subsequent test, in this way Kq qualifies as a valid K1c result. This is expressed as

$$Kfmax \leq \alpha(\sigma_{y1}/\sigma_{y2})Kq. \qquad (14)$$

ASTM E-399 determined that α should be 0.6 while BS 5447 has a more relaxed value of 0.7 for α. These values are presumably based on experiments by Brown and Srawley (1970) for the ASTM E-399 and by May (1970) for BS 5447. The σ_{y1} and σ_{y2} are the yield stresses at the temperature of fatigue precracking and of fracture testing respectively. This is incorporated to ensure that the plastic zone sizes are compared correctly. Realizing that the Kfmax value can only be computed if the K1 or Kq value to be obtained has been estimated, the ASTM E-399 provides an additional guideline for estimating Kfmax such that

$$Kfmax/E \leq 0.002\sqrt{in} \quad . \qquad (15)$$

A further restriction is that the stress ratio R during fatigue precracking should be between 0 and 0.1 for BS:5447 and should be between -1 and 0.1 for ASTM E-399. This unexplained R-ratio restriction maximizes the crack propagation rate in fatigue precracking.

3.2.2 COD Standard (BS 5762:79)

Since the derivation of the COD measurement can be made even when there is considerable plastic flow ahead of the crack, unlike the K1c method, specimens of available thickness of interest can be used.

To simulate severe defect possible, a fatigue precrack is induced in the COD specimen. The standard specifies the Kfmax value so that the plane strain plastic zone size during fatigue precracking remains 50 times smaller than the specimen thickness, B. The derivation is as follows;

$$r_y \simeq B/50 \qquad (16)$$

Where r_y is the plastic zone size during fatigue precracking related to the specimen width. Equation 6 gives the plastic zone size in terms of the stress intensity factor K1 and the yield strength. For a minimum, the plane strain value of r_y is used. Combining Eqn.6 and Eqn.16 and replacing K with Kfmax gives

$$\{1/6\pi\}(Kfmax/\sigma_y)^2 \simeq B/50$$

or

$$Kfmax \leq 0.63\ \sigma_y \sqrt{B}. \qquad (17)$$

An alternative derivation of the above equation can be obtained from Eqn.13, where Kfmax replaces K1c. Although not specified, it is reasonable to assume that σ_y refers to the yield strength at the fatiguing temperature.

For the remainder of the procedures the COD standard has adopted the procedures included in BS 5447 for K1c. This includes the restriction on R-ratio.

The standard specifically states that if the subsequent test has its fracture value close to the linear range of the load-displacement curve, the secant offset procedure shall be applied to test whether a valid K1c measurement can be made.

3.3 Fracture Test

3.3.1 K1c Fracture Test (ASTM-E399; BS 5447)

When the specimen has been precracked in fatigue to obtain a/W values in the range of 0.45 - 0.55, the fracture test is carried out either in tension or bending. For a bend test the total loading span is 4W. Specimen inspection is required before testing to fracture, this includes measurement of thickness B and width W to the nearest 0.1%W on a line not further than 10%W away from the crack plane.

These values of B and W are used as a basis when determining the validity of the test after fracture, eg: checking the length of fatigue crack a to ensure that its average taken at three position of 25%, 50%, 75%B is within the constraint on a/W described above.

Testing to fracture is done with a loading rate such that the rate of increase of stress intensity factor is within 30 to 150 ksi√in per minute. For the bend test the method specifies a requirement for a roller support to avoid friction upon loading. An example of a clip-gauge design for displacement measurement is also given in the standards. The recorded load-displacement curve should have a slope between 0.7 and 1.5 for its linear part. This is to minimise the error that might be created from the 5% secant method in determining the critical load Pq.

Typical load-displacement curves are shown in Fig.9. A line with a slope 5% less than the slope of the tangent OA to the initial part of the record is drawn, then a load P_5 is obtained. Pq is equal to P_5 or any higher force that precedes P_5.

When a valid Pq has been obtained the Kq value can be calculated. The standards provide equations for both the bend test piece (Eqn.5) and tensile test piece. Alternatively, a table is given for each case to relate Pq to Kq. The Kq then becomes K1c when the factor $2.5(Kq/\sigma_y)^2$ is less than both the thickness of the test piece and the crack length and the other validity criteria are met.

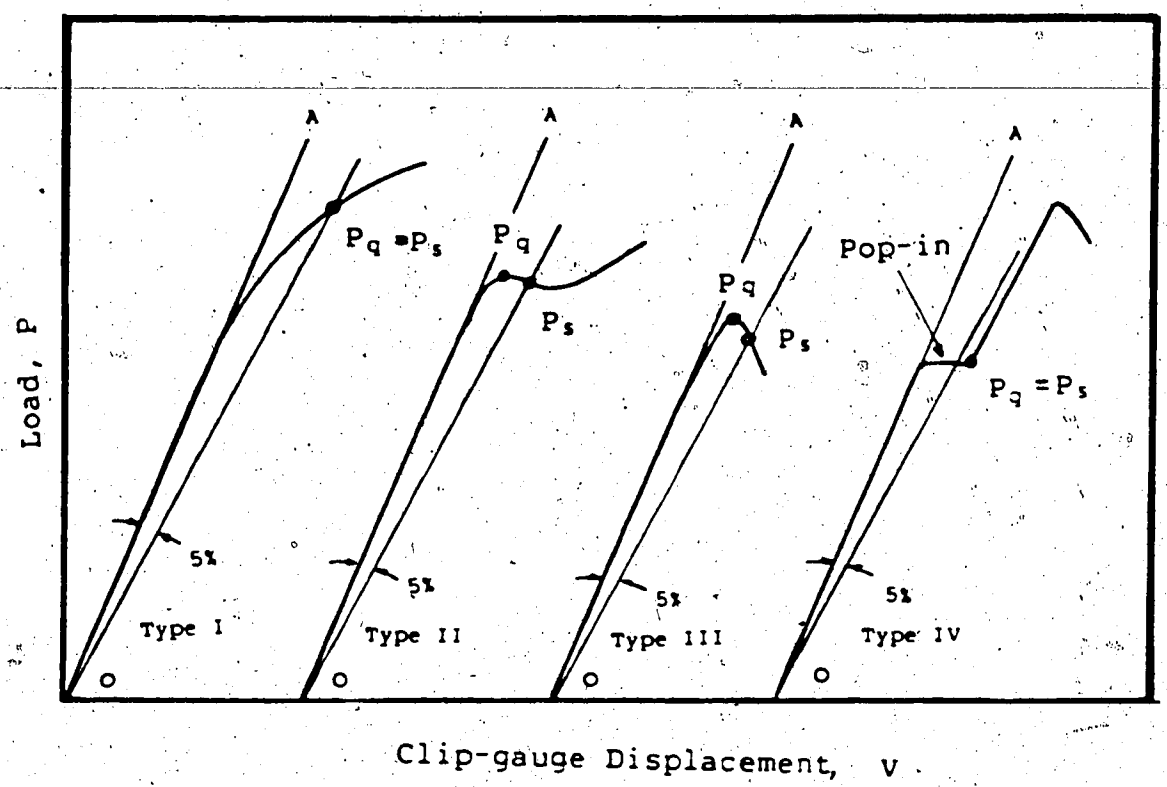

Figure 9 Typical load versus clip-gauge displacement curves for K1c test

3.3.2 COD Fracture Test

As with the K1c method, the COD standard requires accurate measurement of specimen dimensions after fatigue precracking. The results are to be used as a basis in determining the validity of the subsequent test.

The requirement for a roller support, clip-gauge for displacement measurement and loading rate range are all adopted from K1c standards.

Typical load-displacement curves are shown in Fig.10. From these curves, the COD for initiation, critical, unstable and maximum crack growth can be obtained. These are termed δi, δc, δu and δm and are expressed as

$$\delta i,\ \delta c,\ \delta u \text{ or } \delta m = \{K^2(1-\upsilon^2)\}/2\sigma_y E + \{0.4(W-a)Vp\}/\{0.4W+0.6a+Z\} \quad (18)$$

where K is expressed as

$$K = YP/BW^2 \quad (19)$$

The COD standard gives a value for Y with the corresponding a/W ratio. P and Vp are the force and plastic component of clip-gauge opening displacement respectively, which correspond to the relevant values of Vi, Vc, Vu or Vm (see Fig.10). Notice that Eqn.18 is a combination of Eqns.10 and 11. The reason is that Vp is used instead of V and is measured relative to the linear clip-gauge displacement. For type III, IV and V, the multiple specimens technique will have to be used to determine the initiation value of δi.

3.4 Effect of Kfmax on K1c and COD

3.4.1 Effects of Kfmax on the K1c

In preparing the fatigue crack the value of Kfmax is limited by Kfmax $\leq \alpha$ Kq. Experiments have shown that Kq increases when a high Kfmax exceeding the limiting value of

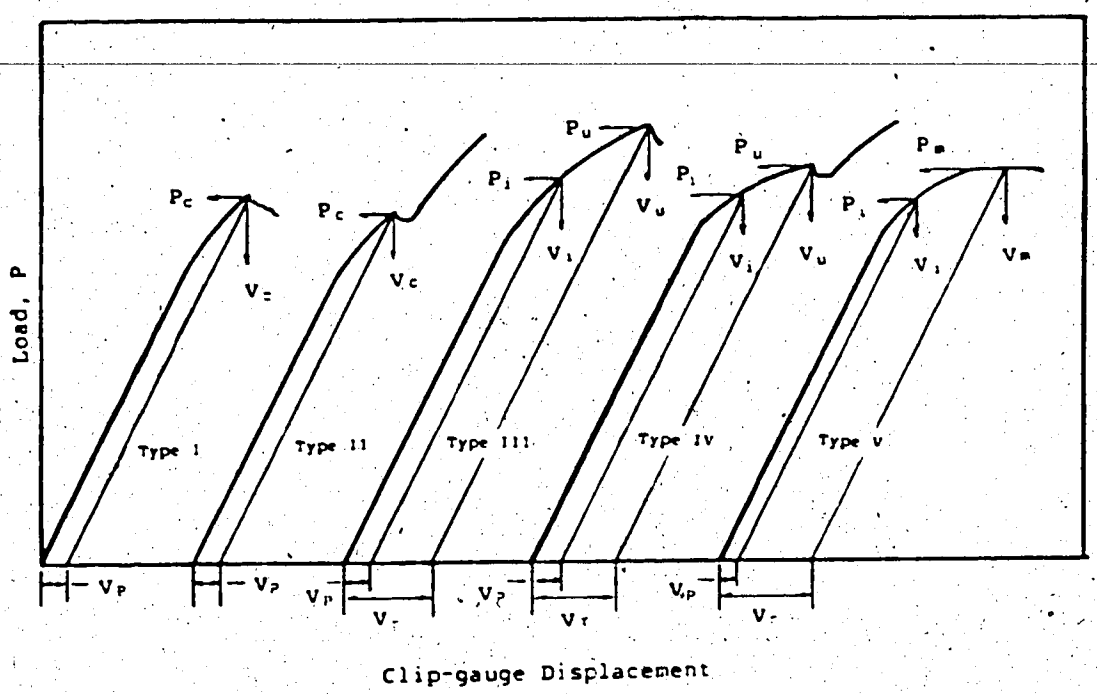

Figure 10 Typical load versus clip-gauge displacement curves for COD test

αK_{1c} is applied (Fig.11). Various researchers have determined values of α ranges between 0.5 to 0.9, depending on the material being tested.

Brown and Srawley (1970) determined α=0.6 on 18Ni grade 30D maraging steel. This value has been adopted by ASTM standard E-399. May (1970) determined α=0.67 for high strength carbon martensitic Ni-Cr-Mo-V steel. This value has been simplified to 0.7 in the adoption by BS 5447. Kaufman and Schilling (1973) and Kaufman (1977) found that for

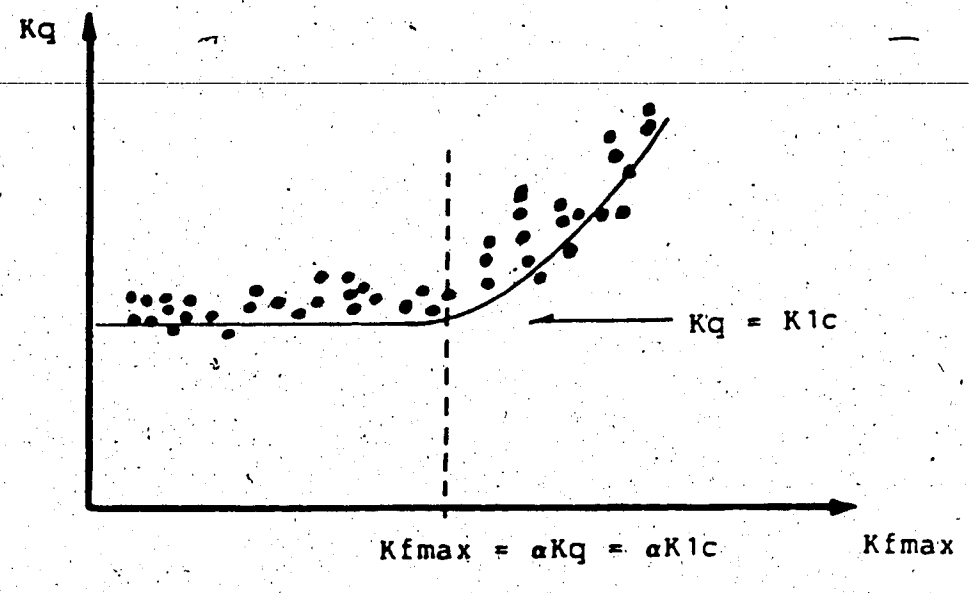

Figure 11 Effect of Kfmax on Kq (typical experimental results)

aluminum alloys α as high as 0.8 could be used. Clark (1979) for 3Ni,1Cr,0.5Mo gun steel and Yeh and Burck (1979) for AISI 4140 steel concluded that for high strength steel α had to be limited to 0.5.

Kaufman (1977) suggested that the value of α imposed by E-399:1981 should be relaxed to 0.8 for aluminum alloys. Jones and Brown (1977) were of the opinion that 'special relief procedures' should not be incorporated into ASTM E-399 for specific materials. If this latter opinion is correct the data by Clark (1979) also Yeh and Burck (1979) indicate that α should be reduced to 0.5 from the current value of 0.6 and 0.7 in ASTM E-399 and BS 5447 respectively.

Several explanations have been offered by researchers for the influence of Kfmax on Kq. The more widely accepted explanations include the following:

a)Crack Closure

The crack closure theory replaces ΔK with effective ΔK ($\Delta Keff$), taking account of residual compression at the crack tip. Higher Kfmax values result in higher crack closure levels. Elber (1971) gave a crack closure model that was slightly modified by Towers (1981) as shown in Eqn.20.

$$Kq = Kql + (0.5 + 0.1R + 0.4R^2)Kfmax \qquad (20)$$

where Kql is the lowest possible value of Kq.
The crack closure model by Maddox et al (1978) was also presented in a different form by Towers in Eqn.21.

$$Kq = Kql + (0.14 + 0.86R)\ Kfmax \qquad (21)$$

In both of the above relations the value of Kq increases with Kfmax and R. Experiments by Towers did not verify the above expressions.

b)Cyclic hardening and softening (reversed plastic zone)

It has been observed that material which demonstrated the greatest sensitivity of Kq to Kfmax also demonstrated pronounced cyclic softening. Indication of cyclic softening

is given by the ratio of the material's ultimate to yield stress (σ_m/σ_y). The lower this ratio is the greater the influence of the cyclic softening (Table 1).

Towers (1981) reasoned that the increased sensitivity of Kq to Kfmax with cyclic softening was presumably because the softening effectively improved the fracture toughness of the material. Roman et al (1981) commenting on the critical stress model of cleavage fracture showed that cyclic softening increased Kq where cyclic hardening decreased it.

Table 1 Indication of cyclic softening by the ratio of the material ultimate to yield stress.

	α	σ_m/σ_y	Material
Clark (1979)	0.5	1.08	3Ni,1Cr,0.5Mo gun steel
Brown and Srawley (1970)	0.6	1.03	18Ni grade 30D maraging steel
Kaufman and Schilling (1973)	0.8	1.15→1.25	2014-T6 aluminum
May (1970)	0.8	1.25	EN-30B steel
Towers (1981)	0.7	1.45→1.51	BS 4360-50E steel

In general σ_m/σ_y <1.2 should show a pronounced cyclic softening effect and σ_m/σ_y >1.4 should show a cyclic hardening effect (Smith et al, 1963). These indications

however are not sufficientlly sensitive to permit selection of a suitable value for α.

c)Insufficient specimen dimension to maintain plane strain

All standards require specimen dimensions a,B and W/2 to be greater or equal to $2.5(K1c/\sigma_y)^2$. This is to ensure that the specimen dimensions are about $2.5x6\pi r_y$ or about $50r_y$.

A detailed study by Kaufman (1977) concluded that this restriction was adequate for most materials except those of high toughness such as aluminum alloy 2219 T851. In the latter case specimen dimensions of 100 r_y should be used in order to produce a valid K1c.

d)Crack blunting

Higher Kfmax value produce an increase in plastic zone size resulting in a blunter crack tip. The comparison of plastic zone size during fatigue precracking (r_{y1}) with that at fracture (r_{y2}) can be made based on the Kfmax restriction. Applying Eqn.6 and 12, the plastic zone ratio can be expressed as

$$r_{y1}/r_{y2} = (Kfmax/\sigma_{y1})^2/(K1c/\sigma_{y2})^2$$
$$= (\alpha)^2 \qquad (22)$$

Substituting into both the value of α (0.6 and 0.7), the ASTM E-399 and BS 5447 have r_{y1}/r_{y2} of 0.36 and 0.49

respectively. If this plastic zone ratio is the basis of the restriction, a slight difference in α may give a significant change in r_{y1}/r_{y2}. Towers (1981) suggested that an experiment could be done to observe the effect of a high Kfmax on Kq related to crack blunting by a single static preloading before the fracture toughness test.

During the fatigue cycle the crack tip experiences reversed yielding, the plastic zone r_y is superposed by the reversed plastic zone r_{yo} which at a plane strain condition has a value of

$$r_{yo}=\{1/24\pi\}(\Delta K/\sigma_y)^2 \qquad (23)$$

A large reversed plastic zone size could also be responsible for blunting of a fatigue precrack, which would result in a higher Kq value. On the other hand, a higher ΔK value could produce a lower Kq since the fracture toughness would tend to be reduced by the lack of ductility. This uncertainty is further complicated by the effect of cyclic softening or hardening which depends on the σ_m/σ_y value.

3.4.2 Effect of Kfmax on the COD

There has been little study on the effect of Kfmax on COD. Towers in 1981 argued that if the K1c result is affected by Kfmax, on the linear region where the COD result could also be dealt with by a K1c analysis, the COD result should also be affected by the Kfmax.

3.5 Effect of R-ratio on the K1c and COD

The ASTM E-399 standard for K1c requires R to be between -1 and 0.1, while the BS 5447 for K1c and BS 5762 for COD require R to be between 0 and 0.1 . This restriction causes a high crack propagation rate during fatigue precracking. Paris and Erdogan (1963) showed that

$$da/dn = C(\Delta K)^m \qquad (24)$$

Expressing ΔK as $(1-R)K_{fmax}$ (for $K_{fmax} \neq 0$), for a given K_{fmax} value, the fatigue crack propagation rate increases as R decreases.

For a given K_{fmax} value, a higher R-ratio would be expected to produce a sharper crack tip which is closer to the simulated ideal plane crack assumed in the K1 analysis. Limiting $R \leq 0.1$ results in a large ΔK and therefore a large reverse plastic zone. The resulting crack tip is a poor approximation to the ideal plane crack.

Conclusions drawn by Towers from the crack closure theories indicated the opposite of the above argument; that is, Kq is expected to increase with R (Eqn.20,21). Elber's (1971) analysis of crack closure could be intrepreted differently from that of Towers. Since ΔK is replaced by $(0.5+0.4R)\Delta K$, for a constant K_{fmax} the reverse plastic zone size decreases quadratically as R increases (note that the effective ΔK is now equal to $(0.5-0.1R-0.4R^2)K_{fmax}$). The smaller reverse plastic zone size more closely represents

the linear elastic condition at the crack tip.

In an experiment, the study on the effect of R-ratio is difficult to separate from the effect of Kfmax. This is due to the fact that most fatigue machines are unable to keep Kfmax constant as the crack propagates. Further difficulties arise in keeping the R-ratio the same while keeping Kfmax constant. These problems are discussed further in the Experimental Procedure.

4. Acoustic Emission Detection

4.1 Introduction

It has been known for many years that whenever a material undergoes plastic deformation, transient elastic waves are generated due to a rapid release of localized strain energy. Mechanisms that have been proposed as sources of these elastic waves include crack nucleation and propagation, dislocation slip, twinning and grain boundary sliding. Such radiation of elastic waves is known as acoustic emission and can be detected by transducers.

An acoustic emission source generates an expanding spherical wave packet losing intensity at a rate of D^{-2}. When this wave reaches the body boundary, a surface wave packet is created, either Rayleigh or Lamb type wave depending on the thickness. Both wave propagation modes have the advantage that the intensity loss is only inversely proportional to the distance D.

In general, the application of the acoustic emission technique is useful for locating any active defects in large structures when boundary reflections of acoustic waves are negligible (The EWGAE code, 1981; Lenain, 1981). The method is complementary to the ultrasonic method which can discover defects whether active or inactive, only if the defects have a specified minimum size and are appropriately oriented. Once located, the analysis of the acoustic emission provides the engineer with an account of the growing defects.

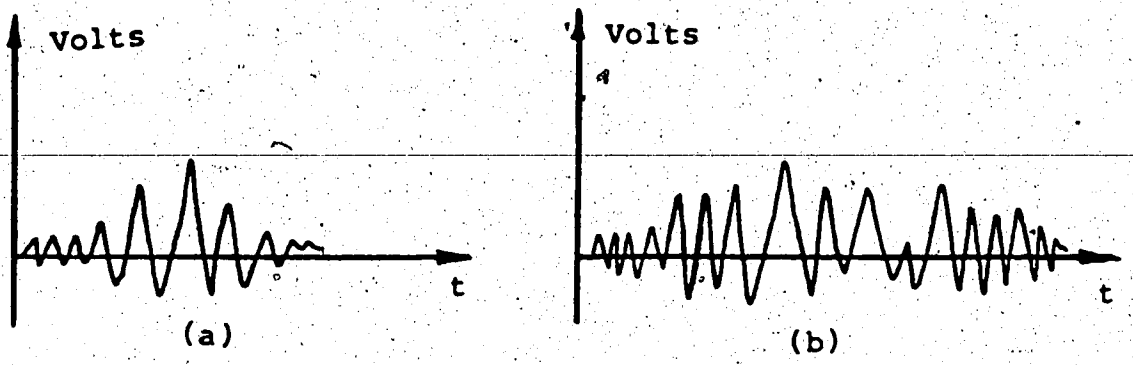

Figure 12 Acoustic emission waveform detected by transducers; (a)burst emission, (b)continuous emission

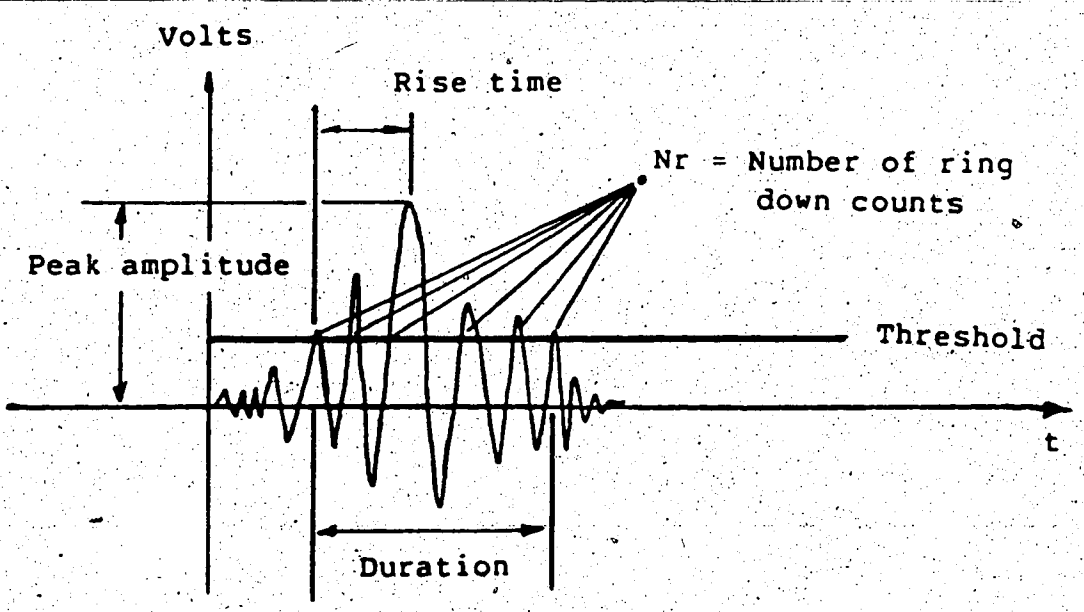

Figure 13 Parameter for characterizing an acoustic emission event

A growing defect may produce either a burst type of emission or a continuous emission (Fig.12). A combination of the two is a very common occurrence. Characterizing acoustic emission events can be done by one of the following methods; counting the number of events, examining the duration of each event, the number of ring down counts per event, energy, peak amplitude or signal rise time (Fig.13).

Measurement of the signal duration is simply done by timing the duration of the first to the last ring down count. Measurement of the number of counts per event can be made if a silent period exists between successive events.

Acoustic emission energy represents the energy that is transmitted by the displacement propagation of the elastic waves. This energy is proportional to the square of the surface displacement that can be detected. Since the output voltage of a transducer attempts to represent this surface displacement, the voltage squared is also proportional to the acoustic emission energy. Energy analysis normally incorporates a squaring circuit and a low-pass filter as shown in Fig.14. The area under the low-pass envelope represents the amount of acoustic emission energy.

In 1972 Radon and Pollock suggested that the relationship between the energy released during the movement of a crack and the length of the crack offered distinct advantages over the usual explanation of crack propagation in toughness test. Harris and Bell (1977) showed that energy measurement of acoustic emission tended to give a larger

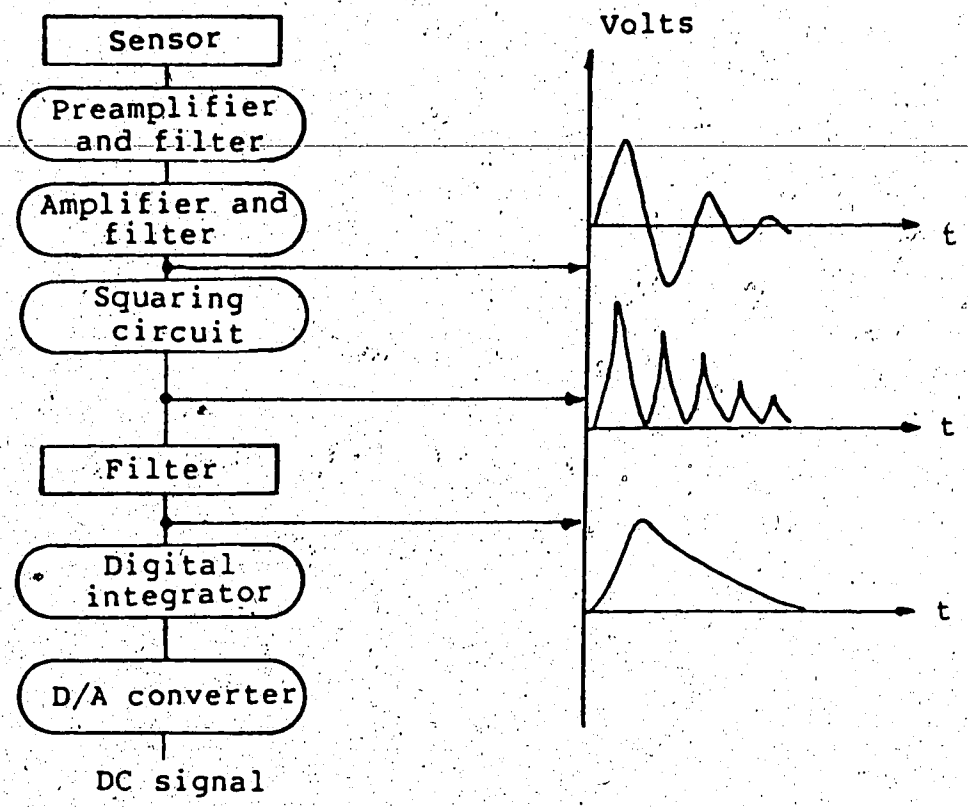

Figure 14 Schematic representation of components in energy measuring device (ref: Harris and Bell, 1977)

weight to a higher amplitude event. Harris and Bell's experiments revealed that energy measurement has no real advantage over the ring down count measuring method in cases in which crack extension is the primary source of acoustic emission.

Advancement in electronics has enabled investigators to discriminate signals from background or unwanted noise. The discriminating methods used are the high-pass and band-pass filter techniques that allow only waveforms with frequencies

of interest to be detected.

A more recent version of a noise discriminator is the measurement of signal rise time. Theoretically, at the source an emitted signal has a rise time approaching zero since it is a pulse. In practice, the recorded rise time is larger due to the system response of the propagating medium and the recording system that includes the transducer and couplants. Background noise caused by pins and fixtures which clamp or hold specimen have significantly greater rise time. The rise time analysis is therefore useful for discriminating signals from this noise.

Higher frequency noise such as electromagnetic waves can also interfere with the acoustic emission signal. Other than using a band pass filter, this noise can be conveniently avoided by turning off the acoustic emission measurement during the time a radio wave receiver is activated by the existence of the high frequency noise (Protasov and Rybin, 1979).

4.2 Acoustic Emission Monitoring of Fatigue Crack Growth

Acoustic monitoring of fatigue crack growth has become an important technique for non-destructive testing. Monitoring crack growth using acoustic emission has been attempted by many researchers, the main problem encountered being the presence of high background noise associated with cyclic loading equipment.

In 1967, Gerberich and Hartbower correlated the incremental fatigue crack area to the summation of acoustic emission energy per incremental crack area. In 1968, Dunegan et al correlated acoustic emission with the stress intensity at a crack front. Their model was based on the volume of plastic zone ahead of the crack. The volume of the plastic zone is proportional to the fourth power of the stress intensity factor K, hence the accumulated acoustic emission count should also be proportional to the fourth power of K. Dunegan's experimental result revealed that total acoustic emission was proportional to the sixth power of K. The discrepency was suspected to be the result of incorrect preloading procedures in the attempt to eliminate acoustic emission near the pin holes of the specimen. Recent unpublished photoelastic studies by Pettett and Budney showed (see Appendix 2) that the preloading procedures suggested by Dunegan et al failed to preload the region at which stresses were concentrated during actual tensile loading.

Harris and Dunegan (1973) observed that acoustic emission can be used for detection of fatigue crack growth as low as 10^{-6} inches per cycle (25.4×10^{-6} m/cycle). The experiment showed that the acoustic emission technique should be suitable for in-service monitoring of a variety of cyclically loaded structures, even in the presence of high background noises. Their acoustic emission detection was done on the upper cyclic load only since this load is

associated with the crack growth. Machine noise was isolated using multilayers of aluminum-steel sheets to produce an impedance mismatch of the propagating noise. Their test results showed correlation of acoustic emission to crack length. Similar experimental results by Morton et al in 1973 showed that there was a better relationship for acoustic emission and the applied range of stress intensity rather than between acoustic emission and the average crack growth rate.

Sinclair et al (1975) incorporated acoustic emission detection for proof testing of the component and during normal stress cycling of the component. Their experimental results revealed that the acoustic emission event count, N, for each cyclic load was related to the stress intensity factor range ΔK and expressed as

$$dN/dn = C\ (\Delta K)^m. \qquad (25)$$

Sinclair et al showed that C and m have similar numerical values to those of fatigue propagation rate parameters described in Eqn.24.

Lindley et al (1978) produced experimental results that showed a relationship of ring down count acoustic emission, Nr, to ΔK described as

$$dNr/dn \propto (\Delta K)^{m \cdot 2}. \qquad (26)$$

Where m is a curve fitting parameter obtained from the crack propagation curve of the material tested. The above relationship was derived originally by Harris and Dunegan in 1973.

4.3 Acoustic Emission Monitoring of Crack Growth and Fracture in Quasi-static Loading

It has been mentioned previously that acoustic emission counts can be related to the stress intensity factor K at the crack tip (Dunegan et al, 1968). Palmer and Heald in 1973 gave an alternative relationship by deriving their equation from Dugdale's plastic zone size (Dugdale, 1960) which allows for a large amount of plasticity at the crack tip. This derivation suggested that $N \propto K^2$. Masounave et al in 1976 suggested that the relationship that was developed by Dunegan et al (1968) should have the exponent value of 11 when it is not corrected for plastic zone but 7 when it is.

Of the many papers written on this subject, of particular interest are the papers by Mitsuru et al (1975) and Clark and Knott (1977) regarding detection of onset of stable crack growth in COD testing using acoustic emission. Takahashi et al (1981) proposed a new acoustic emission procedure for crack growth monitoring in fracture toughness specimens. Their experiments utilized acoustic emission detection of crack initiation during loading in the single specimen J integral method.

5. Experimental Procedure

5.1 Introduction

In this chapter the extent of the experimental research program is detailed. Properties of the test material, relevant specimen preparation technique, and three point bend fracture toughness testing methods are presented. Details of the acoustic emission monitoring during both the specimen preparation (fatigue precracking) and the fracture test are explained.

5.2 Test Material

Five eighths inch (15.875mm) thick quenched and tempered AISI 4140 steel plate was used for all the experimental tests conducted. Microstructure examinations were done to determine the material's rolling direction. Tensile specimens under ASTM E-8:81 designation were made to determine the as-received and the stress-relieved mechanical properties of the steel along its rolling direction. The results are shown in Table 2. Three-point bend specimens were used for both K1c and COD testing using specimens of single size. These specimens were machined with their length in the direction of rolling.

The AISI 4140 as-received condition was tempered to a yield stress of 115 ksi (757 MPa) and having anticipated K1c value ranging from 50 to 70 ksi$\sqrt{in}$ (45 to 64 MPa$\sqrt{m}$). This five eighths inch (15.875 mm) plate was machined to one half

inch (12.7 mm) thick fracture test specimen (Fig.15).

Table 2 Rolling direction mechanical properties of AISI 4140 steel

	σ_y ksi (MPa)	σ_m ksi (MPa)	HRC
As received (Quenched and tempered)	115.5 (797)	139.4 (962)	28
Stress relieved at 1200°F (650°C), furnace cooled	112.1 (774)	137.2 (947)	26.5

Table 3 Chemical analysis of AISI 4140 Steel

C	Mn	P	S	Si	Cr	Mo	V
0.440	0.875	0.019	0.026	0.300	1.020	0.180	0.050

5.3 Specimen Preparation

Three point bend specimens were machined according to ASTM E-399, BS 5447 or BS 5762 standard (Fig.15). The clip gauge mount was machined as shown in Fig.15. As required by BS 5447, after machining and prior to fatigue precracking, stress relieving was done on the fracture specimens at

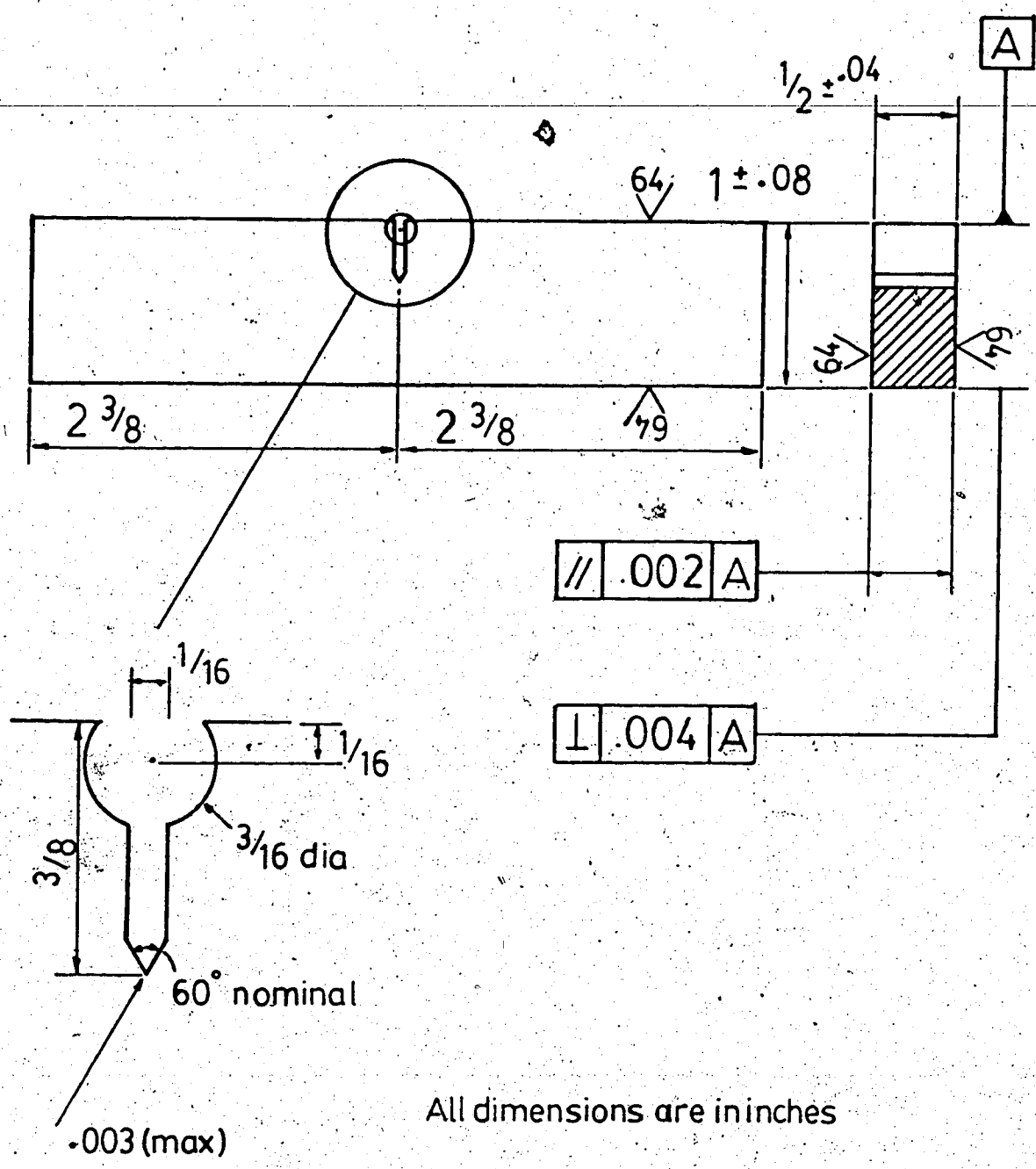

Figure 15 Three-point bending specimen design

1200°F (650°C) for 45 minutes. During the process, the heat treated specimens were covered with grey cast iron chips to avoid scaling on the specimens' surfaces. The specimens were furnace cooled to minimize any development of new residual stresses. The tensile specimens were given the same heat treatment as the fracture specimen to determine the stress relieved mechanical properties. Rockwell C hardness tests were conducted on all tensile specimens, and randomly on fracture specimens to check if there was any difference as the result of heat treatment.

5.4 Fatigue Precracking

Fatigue precracks were developed in the fracture specimens under a variety of maximum bending load and stress ratios (ie: different Kfmax and R ratio values). A target pencil line for a total crack of 0.5W was drawn on each fracture specimen, the precracking was stopped when the crack front reached this line. Based on calculation at the crack length of 0.475W (terminal 5% total crack), Kfmax values ranging from 30 to 70 ksi$\sqrt{in}$ (27 to 64 MPa$\sqrt{m}$) were imposed on different specimens. For each of the Kfmax values, stress ratios of 0.1, 0.3 and 0.5 were used. For each of these combinations, a minimum of five specimens was tested for repeatability. All fatigue precracking was conducted at room temperature with an Amsler Vibrophore resonant fatigue machine set to resonate between 80 to 90 Hz, depending on the stiffness of the bend specimens (ie :

the length of the fatigue crack).

5.5 Acoustic Emission Detection

Experiments were done to test whether or not the machine noise could be eliminated by a combination of a different transducer, filter and gain setting of a Dunegan / Endevco model 3000 system. Experiments using an unnotched specimen showed that the combination of S-750 transducer (750 kHz resonance), 0.3 - 1 MHz band pass filter and 85 dB total gain eliminated all the machine noise. To avoid overloading the acoustic emission system, a resetting circuitry was made, which reset[2] the system every 500 load cycles. Data were recorded a few milliseconds before every resetting. Photographs of the experimental set-up are shown in Figs.16 and 17. The acoustic emission system, the clip-gauge conditioner and the digitizer/recorder are shown in Fig.16. The position at which the acoustic emission transducer and the clip gauge were attached to the specimen are shown in Fig.17.

5.6 Crack Length Measurement

Accurate crack length measurement throughout the fatigue precracking was not the objective of the experiments. The main purpose was to stop the fatigue precracking as soon as the fatigue crack reached a total length of 0.5W approximately. Accurate measurements,

---

[2] Appendix 3 gives the block diagram for the experimental instruments.

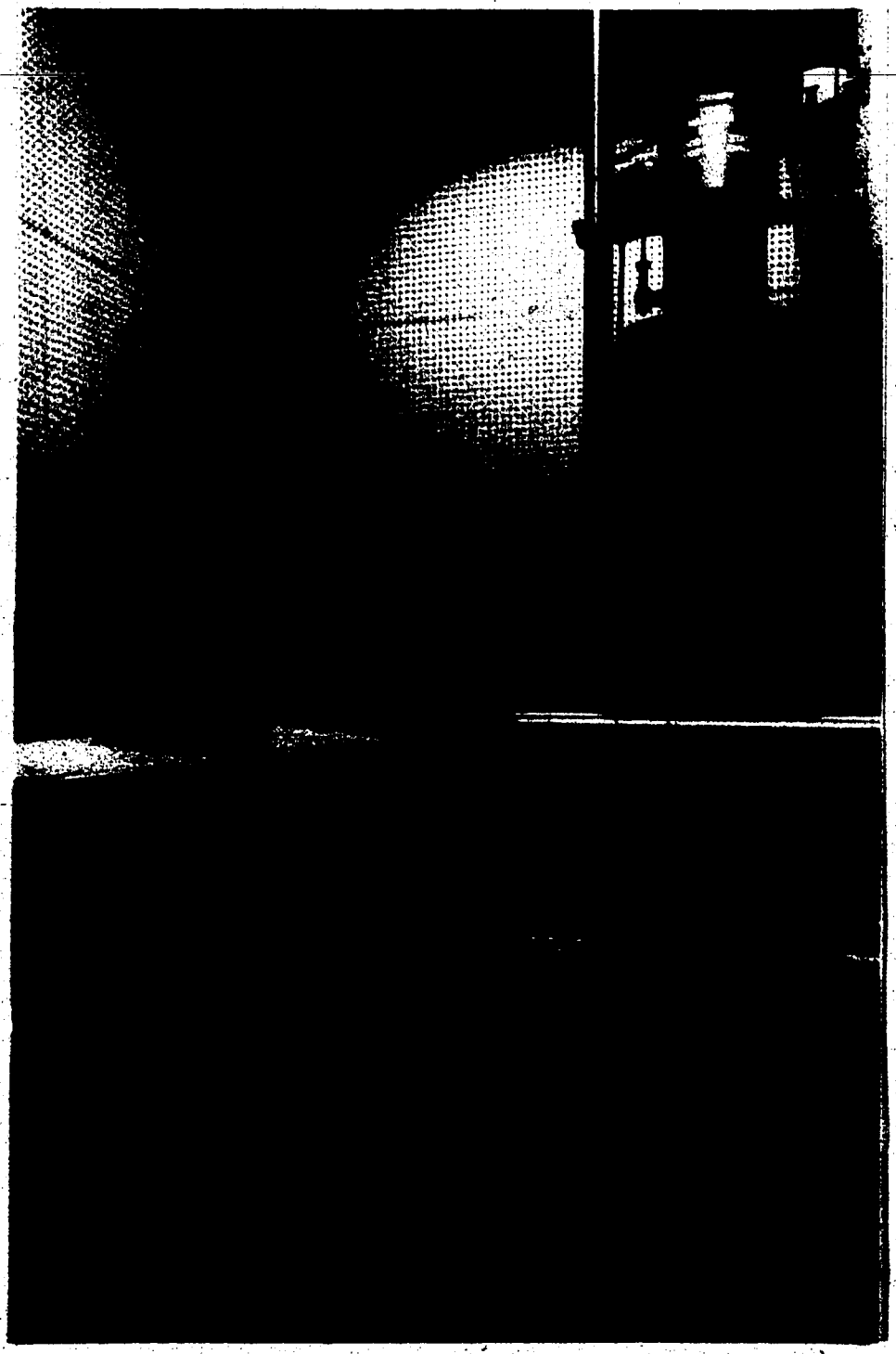

Figure 16 Experimental set-up for monitoring fatigue precracking parameters

Figure 17 Crack length measurement and acoustic emission monitoring a fracture spacimen under three-point fatigue loading

however, were done after the fracture test to determine the value of the average crack length as required by the K1c and COD standards. To provide an approximate value of crack length during fatigue precracking, a clip gauge was used. Using the similar triangle rule, a good correlation of crack length and clip gauge displacement was made (see Appendix 1). Knowledge of crack length throughout the fatigue precracking was useful to monitor the approximate Kfmax value.

5.7 Data Acquisition

During fatigue precracking the mean and maximum loads were monitored. This was to ensure that the minimum deviation from the prescribed load setting could be maintained throughout the fatigue precracking. To obtain an accurate reading of static load and dynamic load, the cyclic load signals were directly taken from the load cell of the Vibrophore machine using a low pass filter and peak detector. Similarly the clip gauge cyclic signals were low-pass filtered to measure the mean displacement which correlated to the crack length as shown in Appendix 1.

For every 500 load cycles, the mean load, maximum load, clip gauge displacement and total acoustic emission were recorded. The recording was done on a Tektronic data cartridge with a custom-built interface as digitizer and controlle for the reset cicuitry. The recorded data were analysed on a mainframe computer (Amdahl 5860). Computer

programs were written for analysis of the recorded data. This included rejection of some tests when the load spectrum indicated that some overloads occured.

5.8 Fracture Toughness Testing

After developing the fatigue precrack at room temperature, the specimen was loaded on an Instron universal testing machine with a loading rate of 0.05 inch/minute (1.3 mm/min) to fracture. This was within the specified loading rate of both K1c and COD standards. The load, clip gauge displacement and acoustic emission counts were recorded for analysis. The K1c and COD evaluation were made from the same load versus clip gauge displacement curve. Computer programs for K1c and COD evaluation were written. Accurate measurement of crack length, specimen dimensions and crack orientation as suggested by the K1c and COD standards were followed.

6. Experimental Results and Discussion

From a total of 117 specimens tested only 98 were considered valid. During the fatigue precracking, some specimens were rejected since overloading occurred for some of the fatigue cycles. This overloading was mostly caused by the difficulties of the Vibrophore machine in following the change of frequency as the crack propagated.

All of the specimens that had been precracked in the controlled conditions were tested to fracture. In meeting the K1c and COD standards eight specimens were considered invalid for reasons of sloping crack-plane and uneven crack-length. The specimens were fatigue precracked with Kfmax value of 30, 35, 40, 49, 56, 70 ksi√in and R-ratio of 0.1, 0.3, 0.5 . For each of the combination the test was repeated five times. The results of the 90 valid tests are presented in this chapter.

6.1 Fatigue Precracking

The preparation of the fatigue precrack needed almost constant attention. The length of time to achieve the total precrack of 0.5W varied from six minutes to two hours, depending on both Kfmax and R-ratio values. Figure 18 shows that for a constant Kfmax value the number of cycles required to reached the terminal cycle (Nt) increased with R-ratio value. The same data was plotted as a function of ΔK in Fig. 19 , which showed that the rate of propagation was a function of the stress intensity range ΔK, a phenomenon

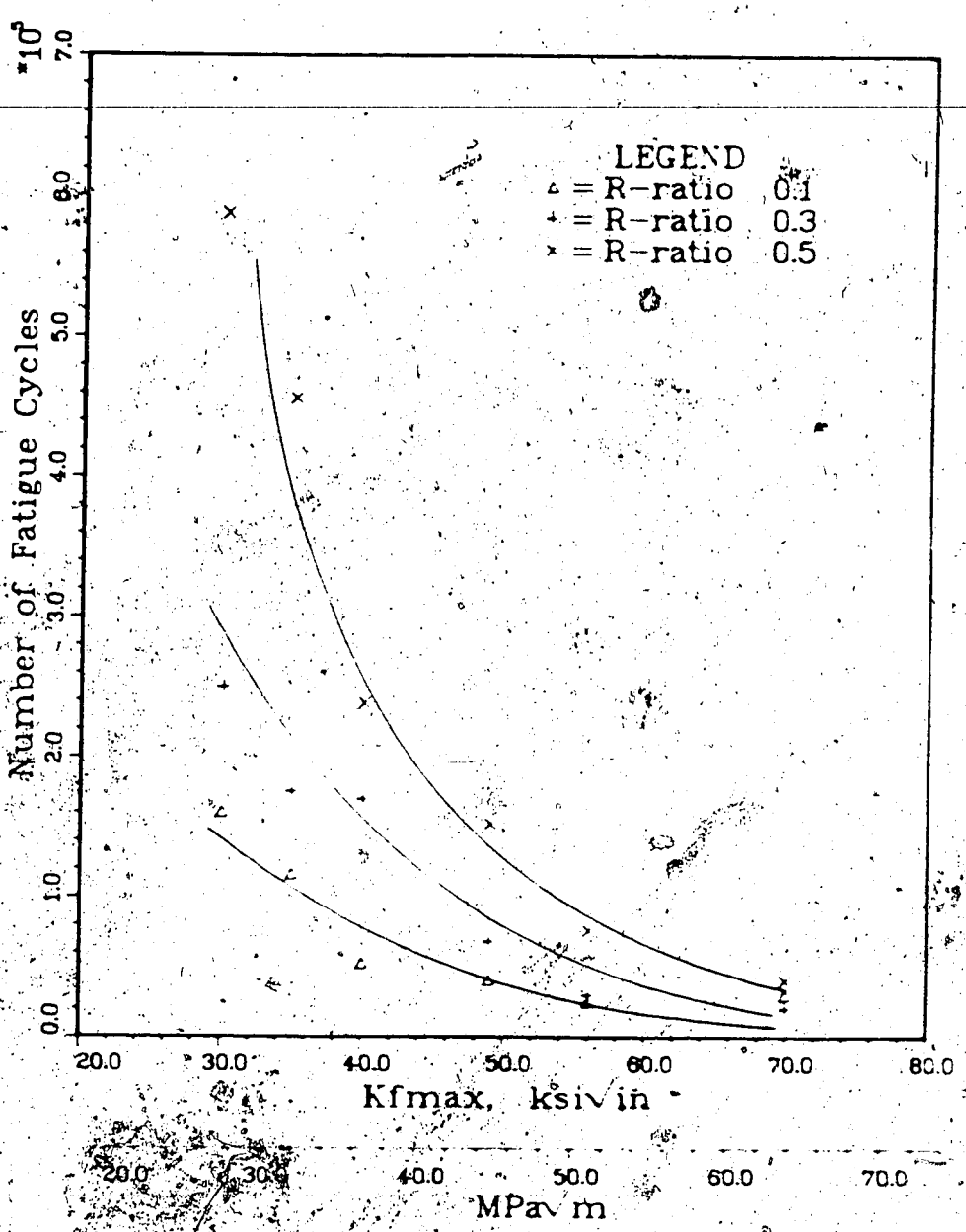

Figure 18 Number of fatigue cycles required to reach 0.5W crack lentgh as a function of Kfmax and R

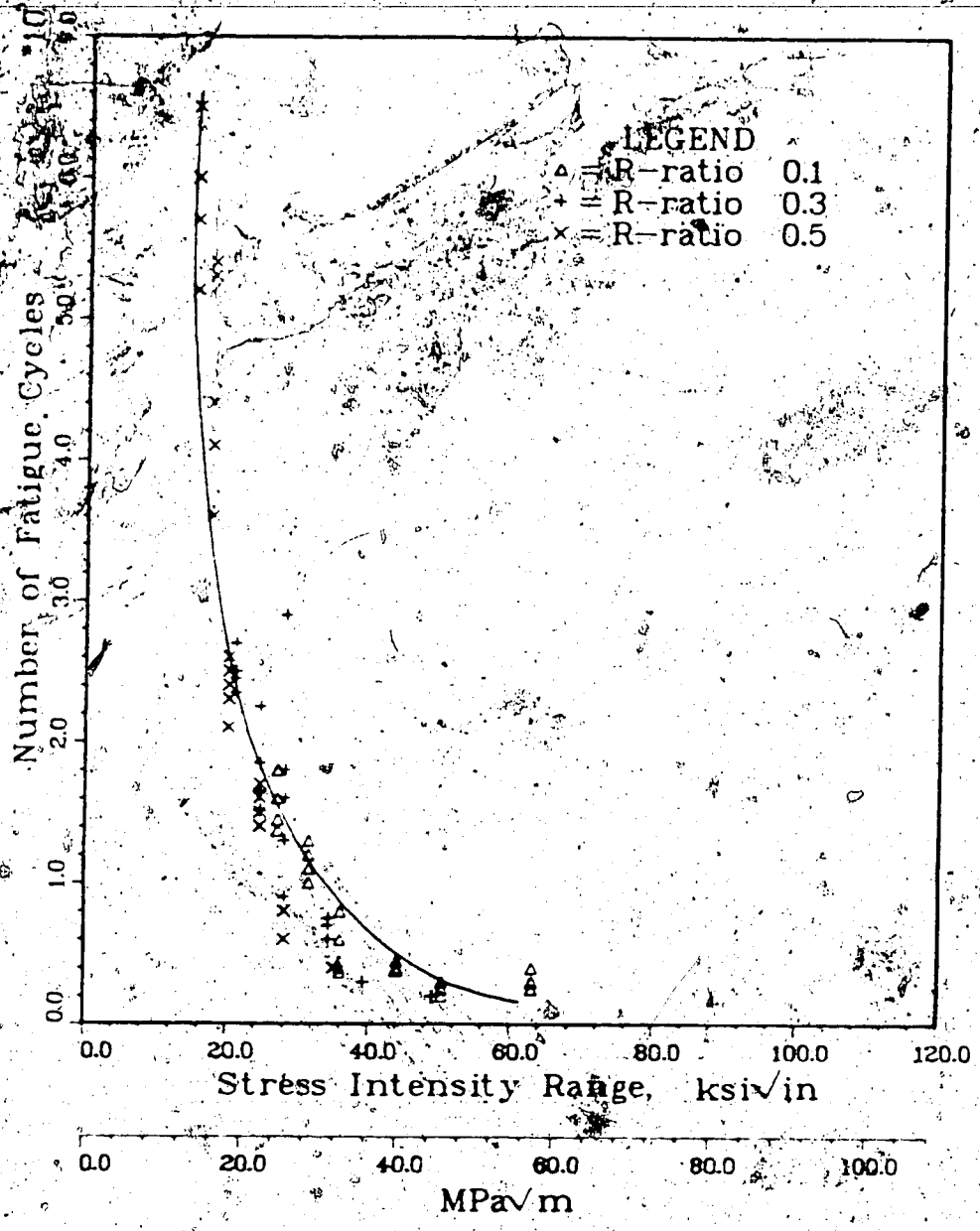

Figure 19. Number of fatigue cycles required to reach 0.5W crack length as a funtion of ΔK

which was observed by Paris and Erdogan (1963). A more common curve is shown in Fig.20, for which the data points were obtained from clip-gauge measuring of the crack length at every 500 load cycles. The curve indicates the crack propagation near the ΔK threshold value. The stress intensity range data was processed from the recorded static and dynamic load and the calculated crack length. A typical curve for the variation of the Kfmax value and the R-ratio value throughout the fatigue precracking is shown in Fig.21. This variation was kept at a minimum by constantly adjusting the static and dynamic load as the crack propagated. A load table was prepared to assist this process. A slight decrease in R-ratio value was observed, mostly at the beginning of the fatigue cycling period. This was caused by mean load overshoot when the Vibrophore machined achieved a resonant frequency. This overshoot occurred at the Kfmax value and resulted in a temporary decrease in R-ratio. The Kfmax value during the terminal 2.5% of total crack length[3] could not be maintained constant, however, increase in Kfmax was within 5% of the expected value.

The crack length and total acoustic emission ring down counts as a function of fatigue cycles are shown in Fig.22. Direct correlation of crack length to acoustic emission was considered poor since the acoustic emission activities were observed to happen at almost random parts of the fatigue

---

[3]The Standards concern with Kfmax value related to the terminal 2.5% of the total crack length ie: between 0.4875W and 0.5W in this test.

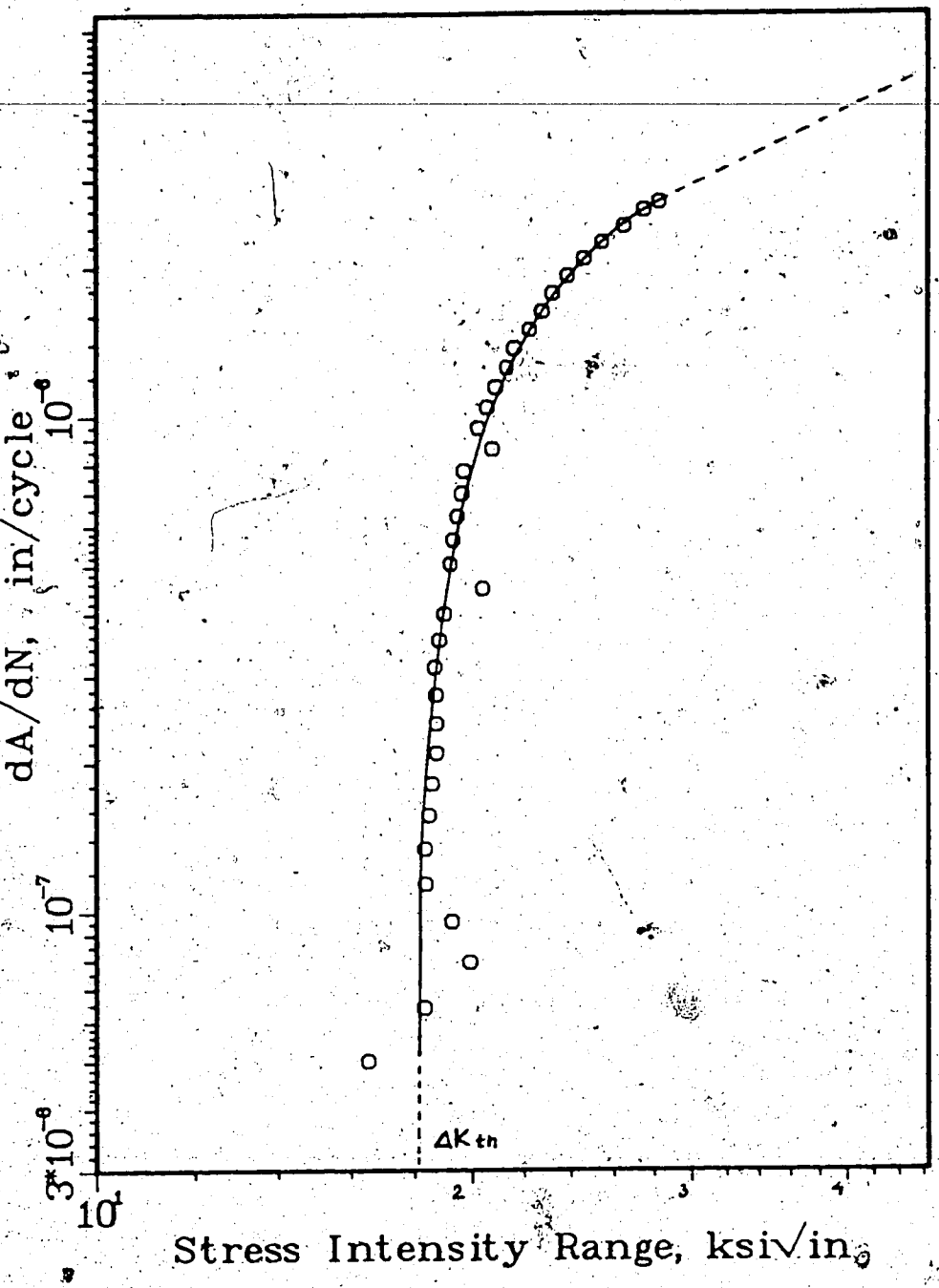

Figure 20. The crack propagation rate of AISI 4140 (specimen C0, σ_y=780 Mpa)

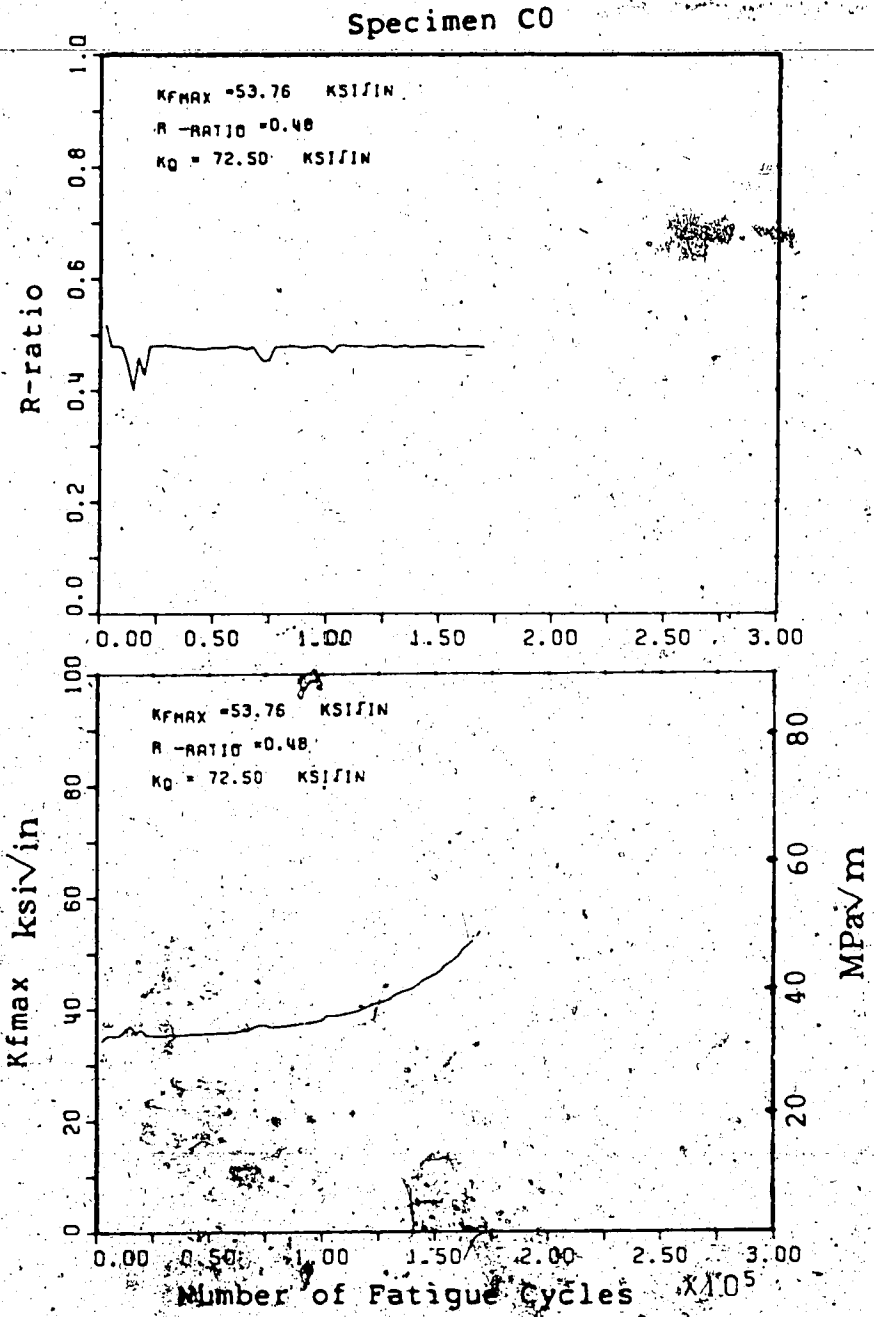

Figure 21 Monitored value of R-ratio and Kfmax during the fatigue precracking

Specimen C0

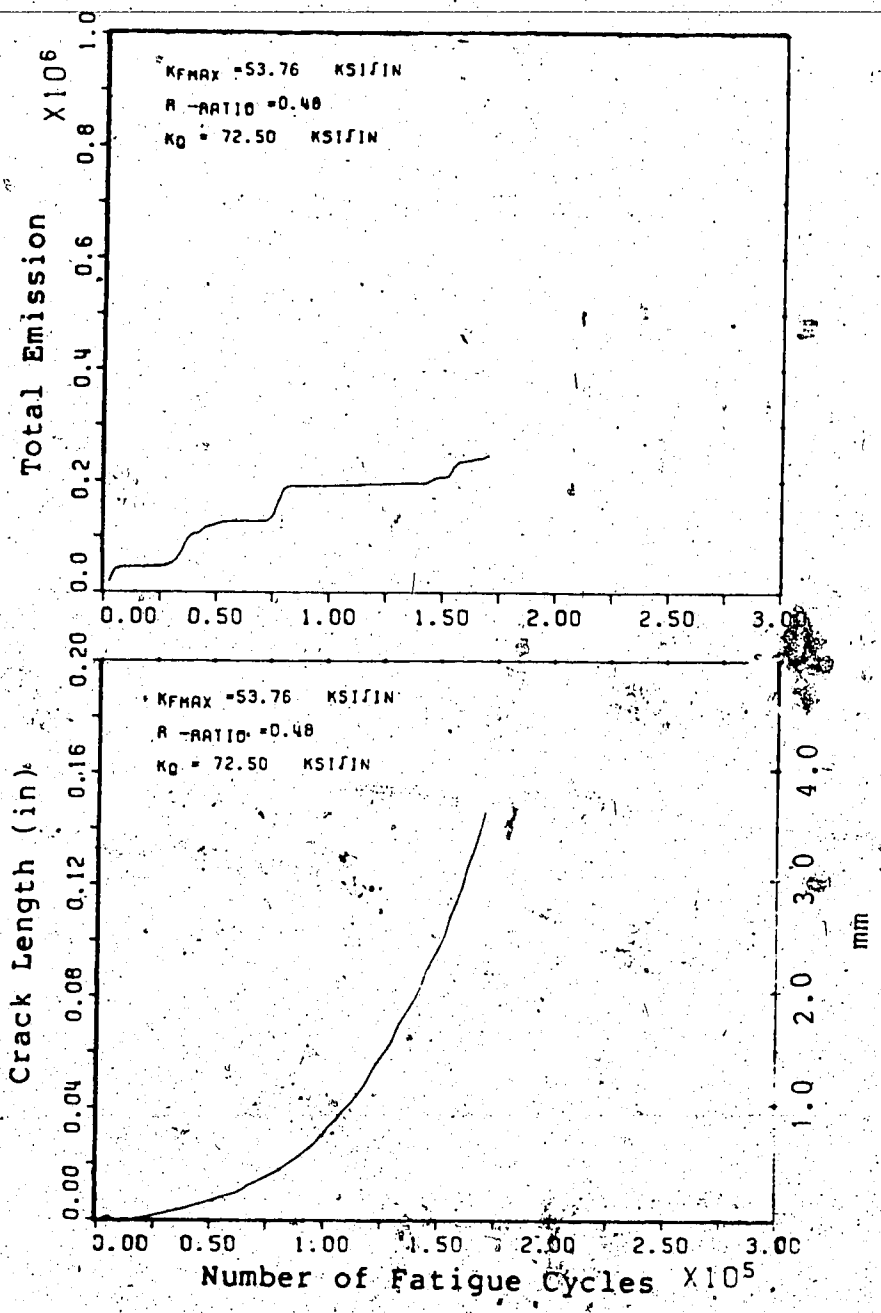

Figure 22 Monitored value of total emission and crack length during the fatigue precracking

history for specimens under the same test constraints. It was observed, however, that the total acoustic emission, for the period of fatigue precracking to reach the 0.5W crack length, was of the same order of magnitude for all specimens. By dividing the total acoustic emission ring down counts (Nr) by the number of fatigue cycles to reach terminal crack length (Nt), an overall average of acoustic counts per cycle was obtained. Figure 23 shows the number of acoustic emission counts per cycle for specimens fatigue precracked at various Kfmax and R-ratio values. The plots show that as expected, the number of acoustic emissions per cycle increased rapidly with the maximum stress intensity factor. This trend was originally observed by Lindley et al (1978) and is described in Eqn.26. The amount of emission was inversely proportional to the R-ratio, which confirmed that for a constant Kfmax the reverse plastic zone size is larger at lower R-ratio resulting in a higher crack propagation rate. The rapid increase of acoustic emission ring down counts per cycle at higher Kfmax and lower R value, suggests that acoustic emission monitoring of fatigue precracking offers comparison of the extent of plastic deformation related to both monotonic and reverse plastic zone. This could later be related to any possible blunting of the fatigue crack.

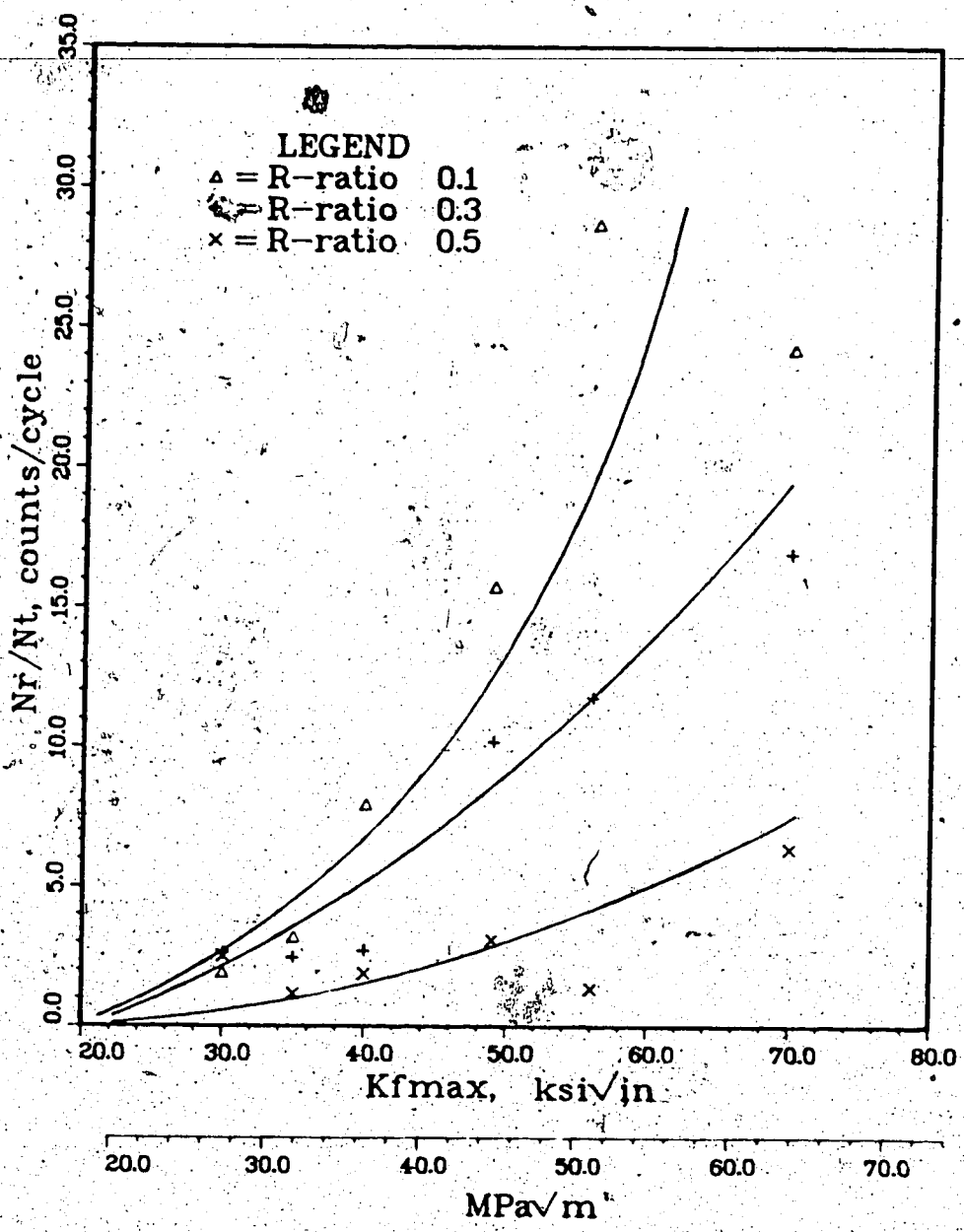

Figure 23 Number of acoustic emission counts per-cycle for differing Kfmax and R-ratio

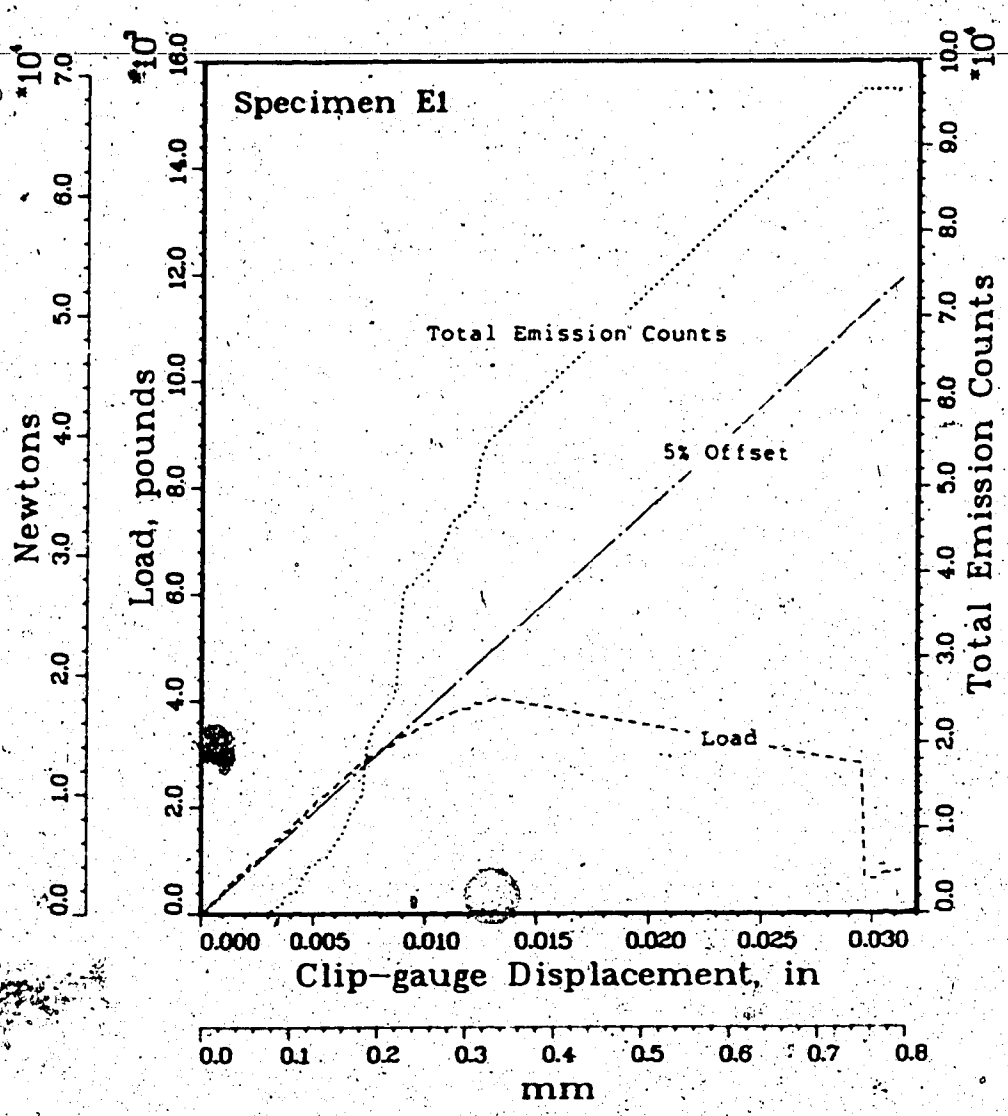

Figure 24a, Typical load also total emission versus clip-gauge displacement of the fracture test; (a)No pop-in, (b)Pop-in occurred

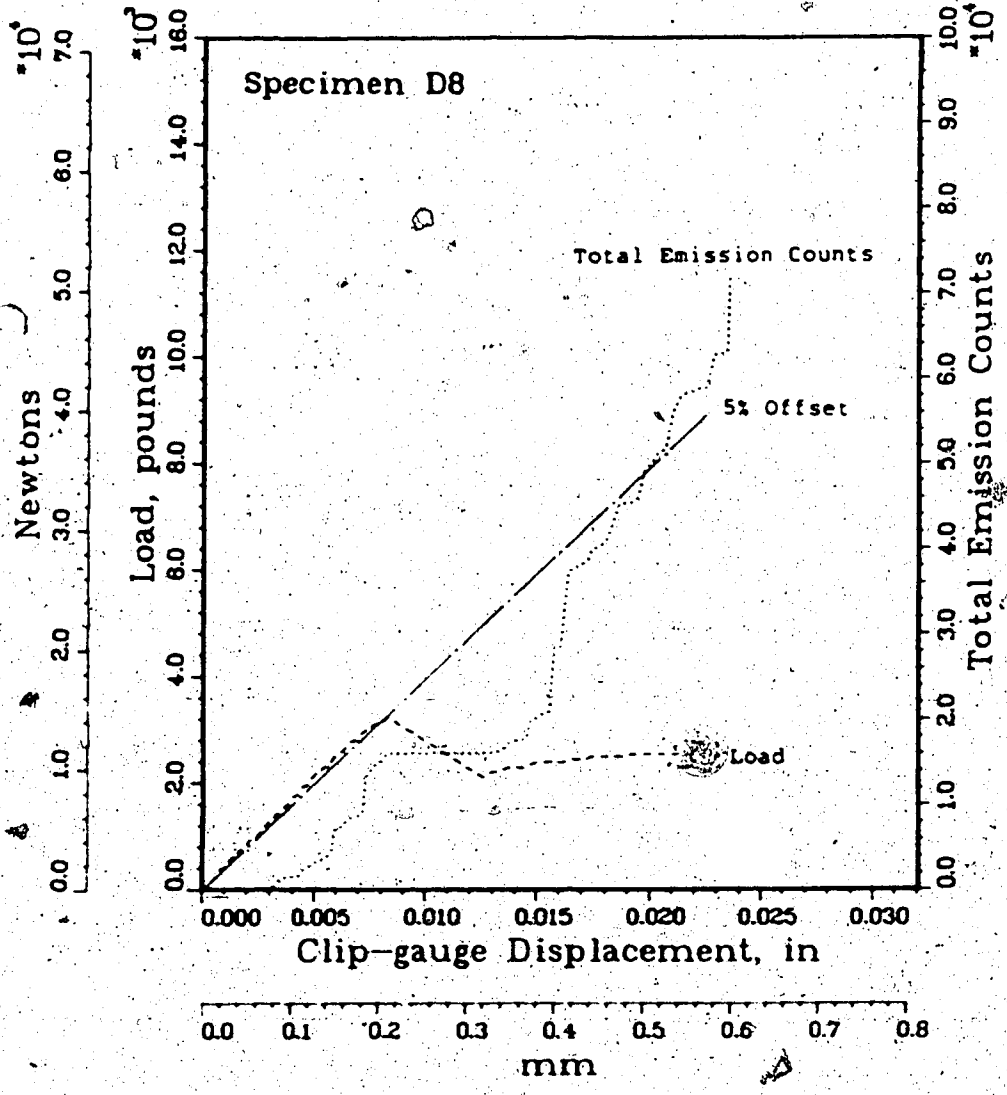

Figure 24 b. Typical load also total emission versus clip-gauge displacement of the fracture test; (a)No pop-in, (b)Pop-in occurred

6.2 Fracture Test

The results of the fracture test are shown in Table 4. A typical curve of load vs clip-gauge displacement is shown in Fig.24. Linear regression was made on the linear part of the curve and the 5% offset line was then calculated. A typical acoustic emission total counts curve is also shown. The rapid rising of total counts is related to the crack tip yielding prior to crack initiation. For the K1c test, only Kq could be presented since the test did not meet the specimen size requirement. The lower value of Kq (Kql) approached 70 ksi√in (64 MPa√m) as indicated by the imaginary line in Fig.25. With this value of Kql, the specimen size required (a, B and W/2) needed to be greater than or equal to $2.5\times(70/112)^2 = 0.97$ inch (24.8mm). This is a factor of 1.94 times larger than the specimen size used in the test. The variation of Kq value with Kfmax and R-ratio is shown in Fig.25. It can be seen that for all R-ratio values, Kq increased with Kfmax, reaching a limit at a higher Kq value. Comparing these curves, Fig.25(d) shows that there was less effect of Kfmax on Kq at the higher R-ratio value. Therefore, for a constant Kfmax, Kq increased with ΔK. Furthermore, the fact that several specimens showed a Kq value as low as 60 ksi√in when fatigue precracked with higher R might suggest that the production of a sharper fatigue precrack was more likely. Alternatively, these lower Kq values could have resulted from material inhomogeneity. The results contradicted the interpretation of the crack

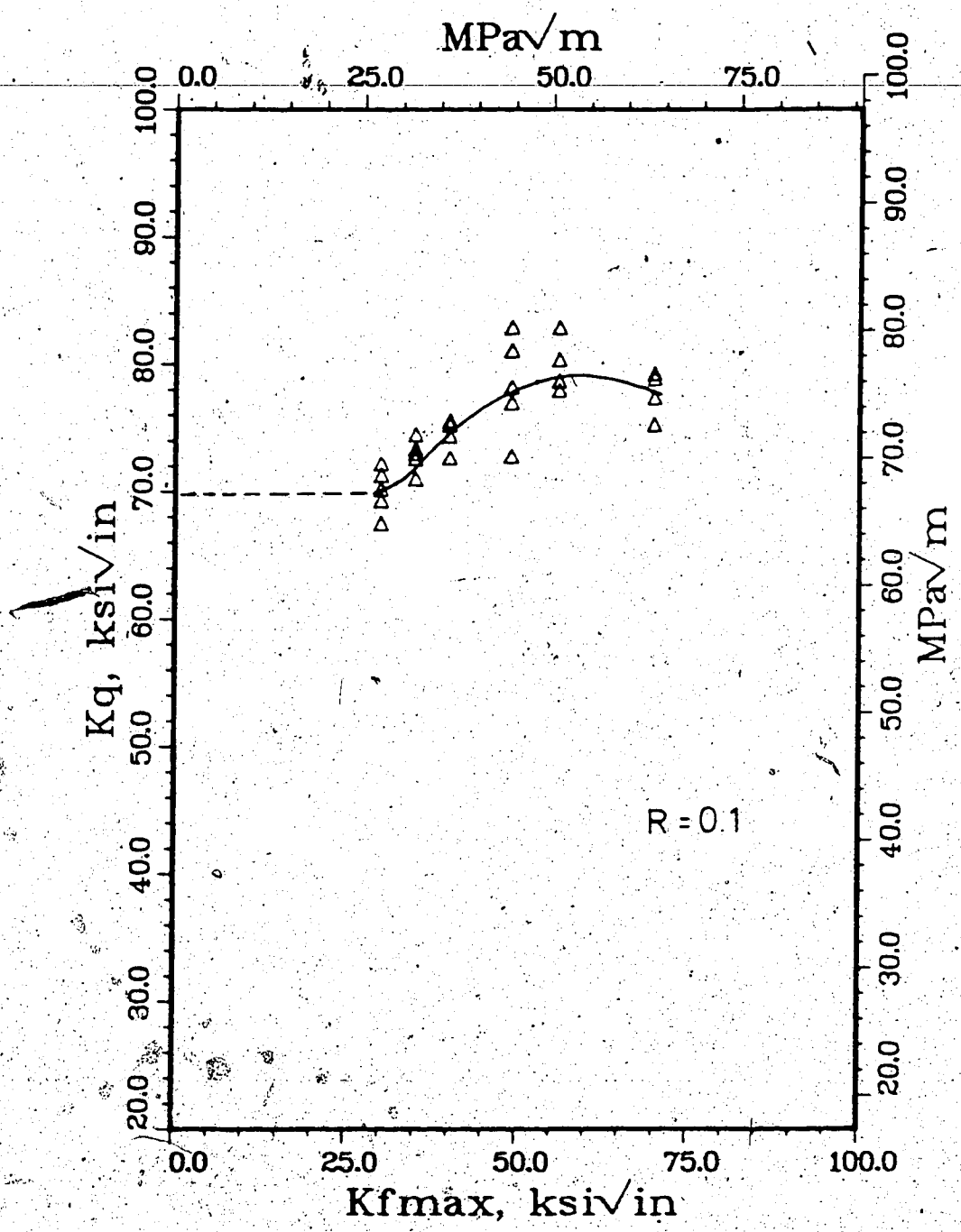

(a)

Figure 25. Effect of Kfmax on Kq at (a)R=0.1, (b)R=0.3, (c)R=0.5 and (d)R=0.1 - 0.5

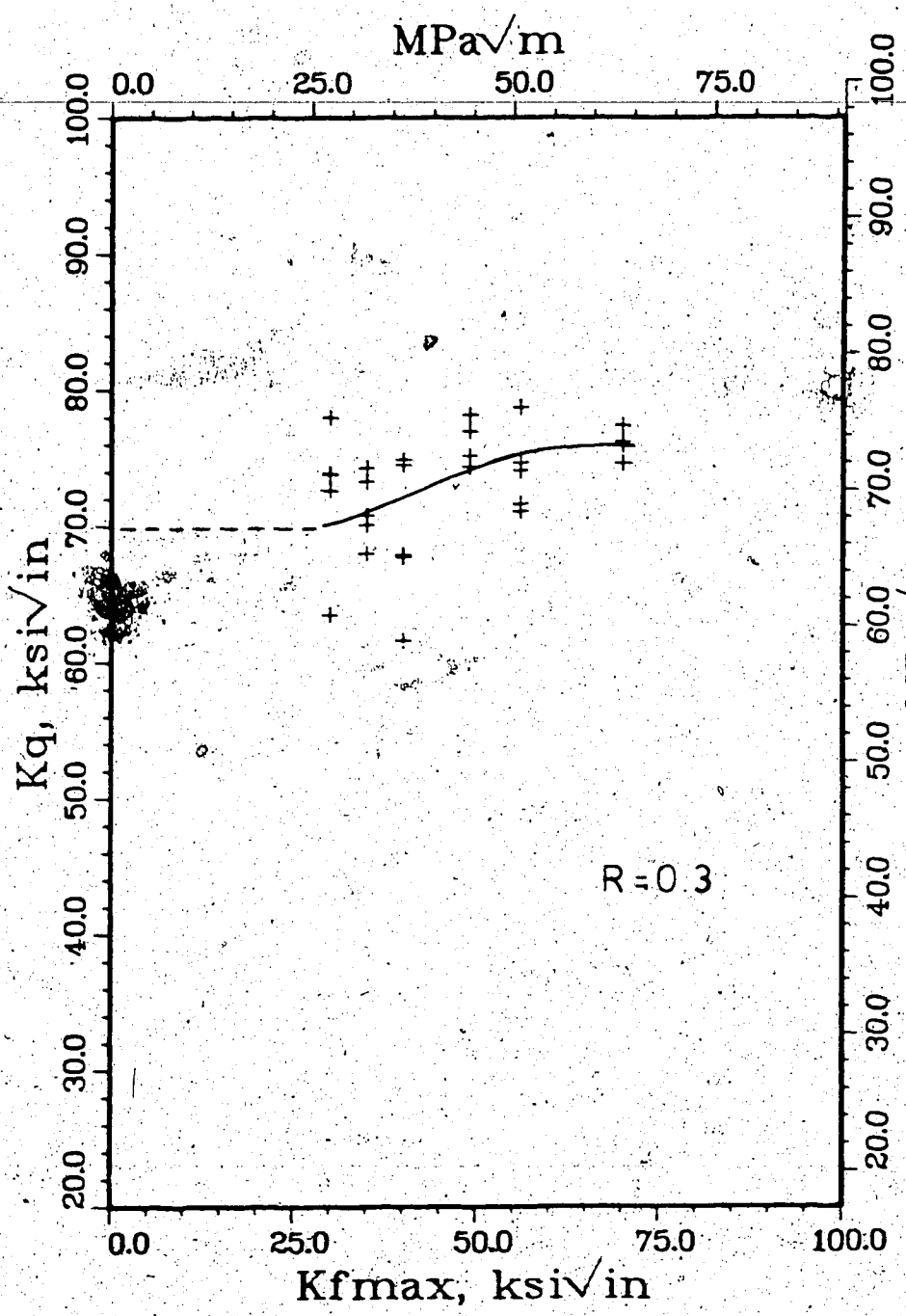
MPa√m
0.0
25.0
50.0
75.0
100.0
90.0
80.0
70.0
60.0
50.0
40.0
30.0
20.0
Kq, ksi√in
MPa√m
R=0.3
0.0
25.0
50.0
75.0
100.0
Kfmax, ksi√in

(b)

Figure 25

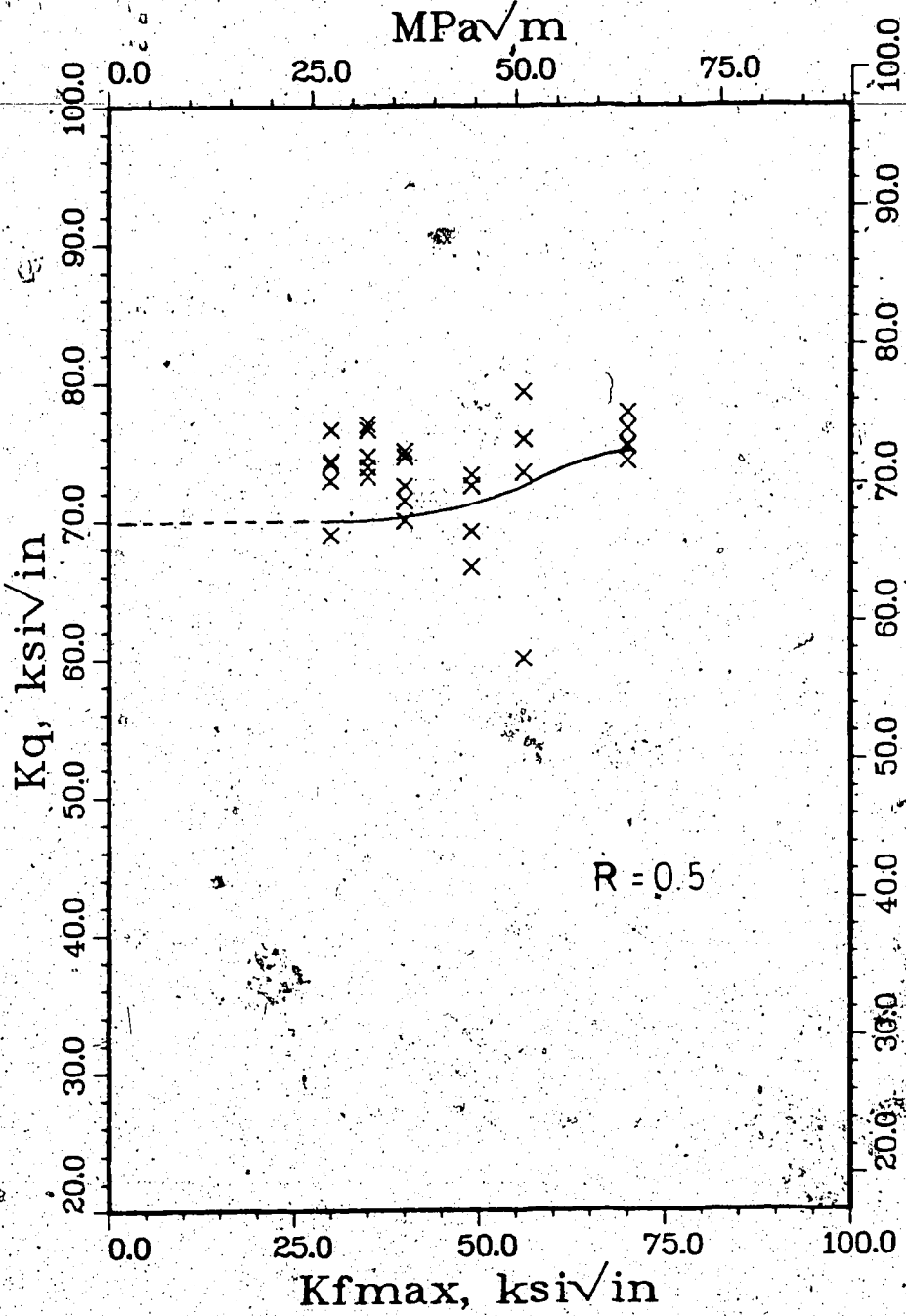
MPa√m
0.0
25.0
50.0
75.0
100.0
Kq, ksi√in
20.0
30.0
40.0
50.0
60.0
70.0
80.0
90.0
100.0
MPa√m
20.0
30.0
40.0
50.0
60.0
70.0
80.0
90.0
R = 0.5
0.0
25.0
50.0
75.0
100.0
Kfmax, ksi√in

(c)

Figure 25

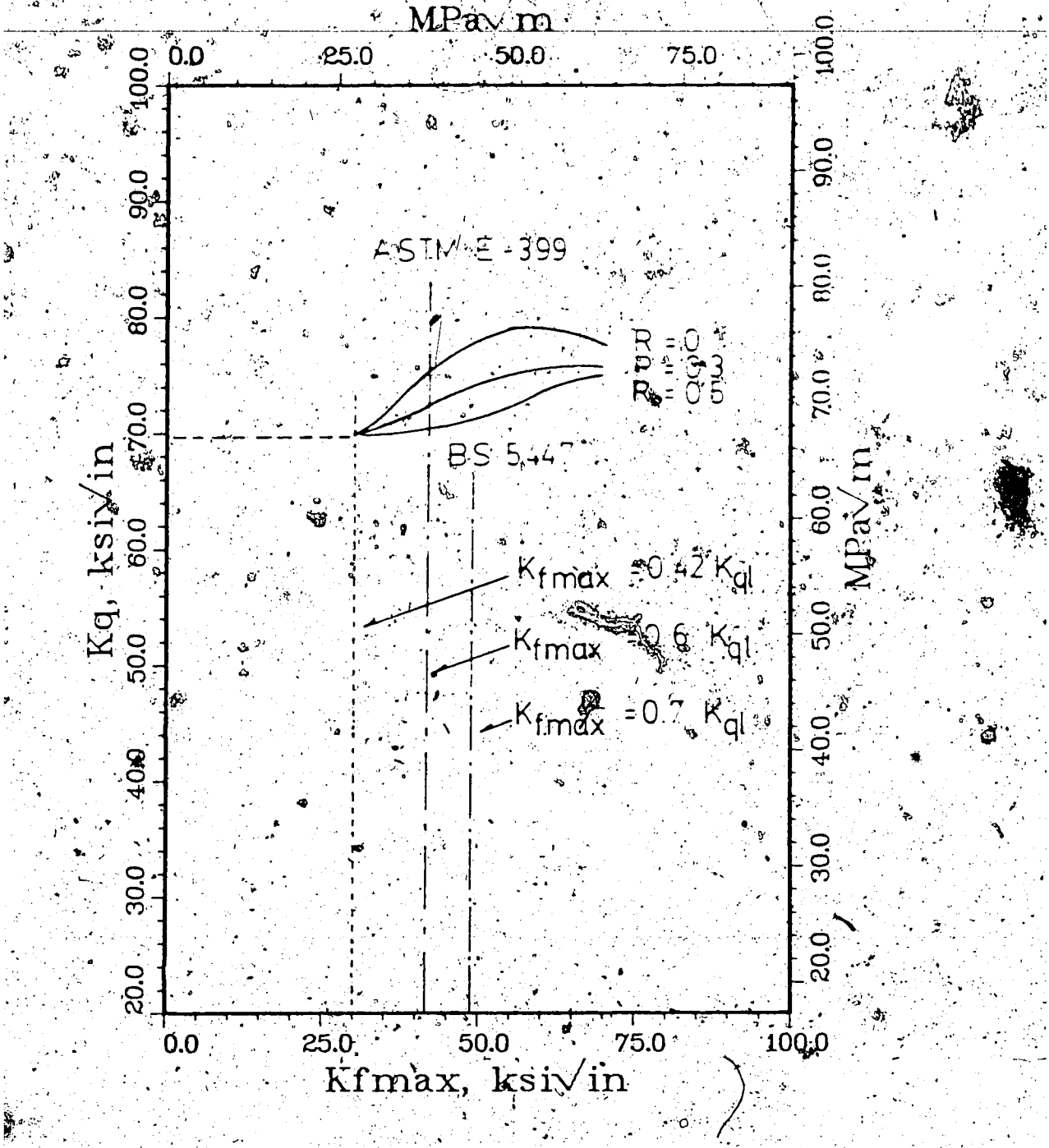
MPa√m
0.0
25.0
50.0
75.0
100.0
90.0
80.0
70.0
60.0
50.0
40.0
30.0
20.0
ASTM E-399
R = 0
R = 0.3
BS 5447
Kfmax = 0.4 Kql
Kfmax = 0.6 Kql
Kfmax = 0.7 Kql
Kq, ksi√in
MPa√m
Kfmax, ksi√in

(d)

Figure 25

closure theory given by Towers in Eqns.20 and 21 and indicates that the crack closure phenomenon may be interpreted as causing a smaller reverse plastic zone size at a higher R-ratio. This is related to the effective ΔK which decreased with increased R-ratio.

The material used in this experiment had an ultimate to yield stress ratio of 1.22. At this value the effect of cyclic softening should not have been present. The results however indicated that the Kc value increased with Kfmax which implied a possible presence of cyclic softening effects. Separate tests to determine the cyclic softening or hardening were not conducted so this assumtion was not confirmed.

For the COD test the fracture toughness was determined as COD maximum (δm). Evaluating the COD initiation (δi) was not done as it required multiple specimens. Presenting toughness in terms of δm in this study was intended to indicate the general trend for the the effect of Kfmax on COD. As shown in Fig.26, δm increased with Kfmax for all R-ratios reaching an upper limit at higher δm. The study on the effect of R-ratio on δm was not strongly conclusive. The result indicated more scatter in δm at higher R. The general trend of the curves are reproduced in Fig.26(d). However, it was observed that limiting R to less than 0.1 did not give any assurance that a sharper fatigue precrack could be produced than when higher R values were used.

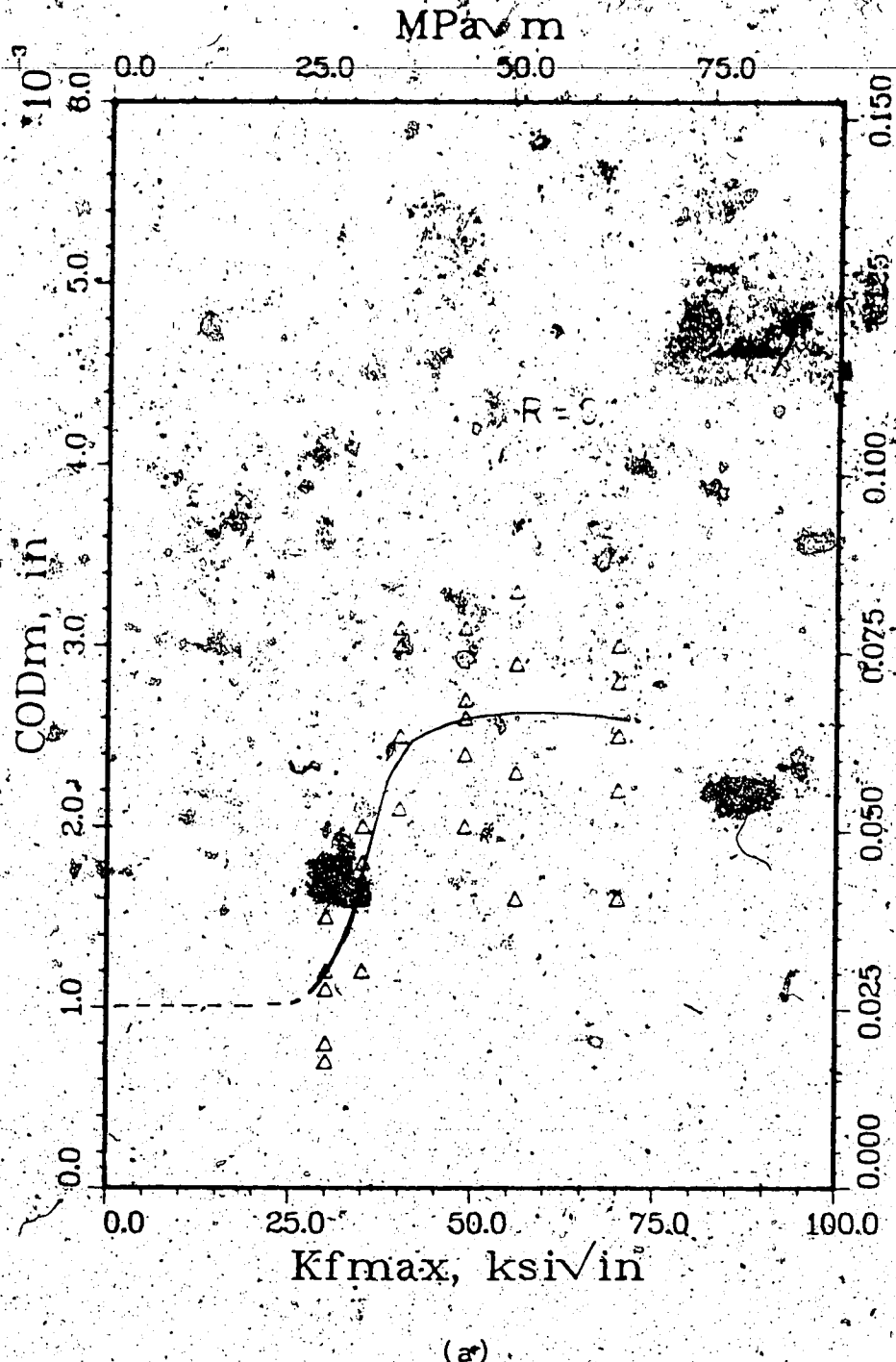

Figure 26 Effect of Kfmax on CODm at (a)R=0.1, (b)R=0.3, (c)R=0.5 and (d)R=0.1 - 0.5

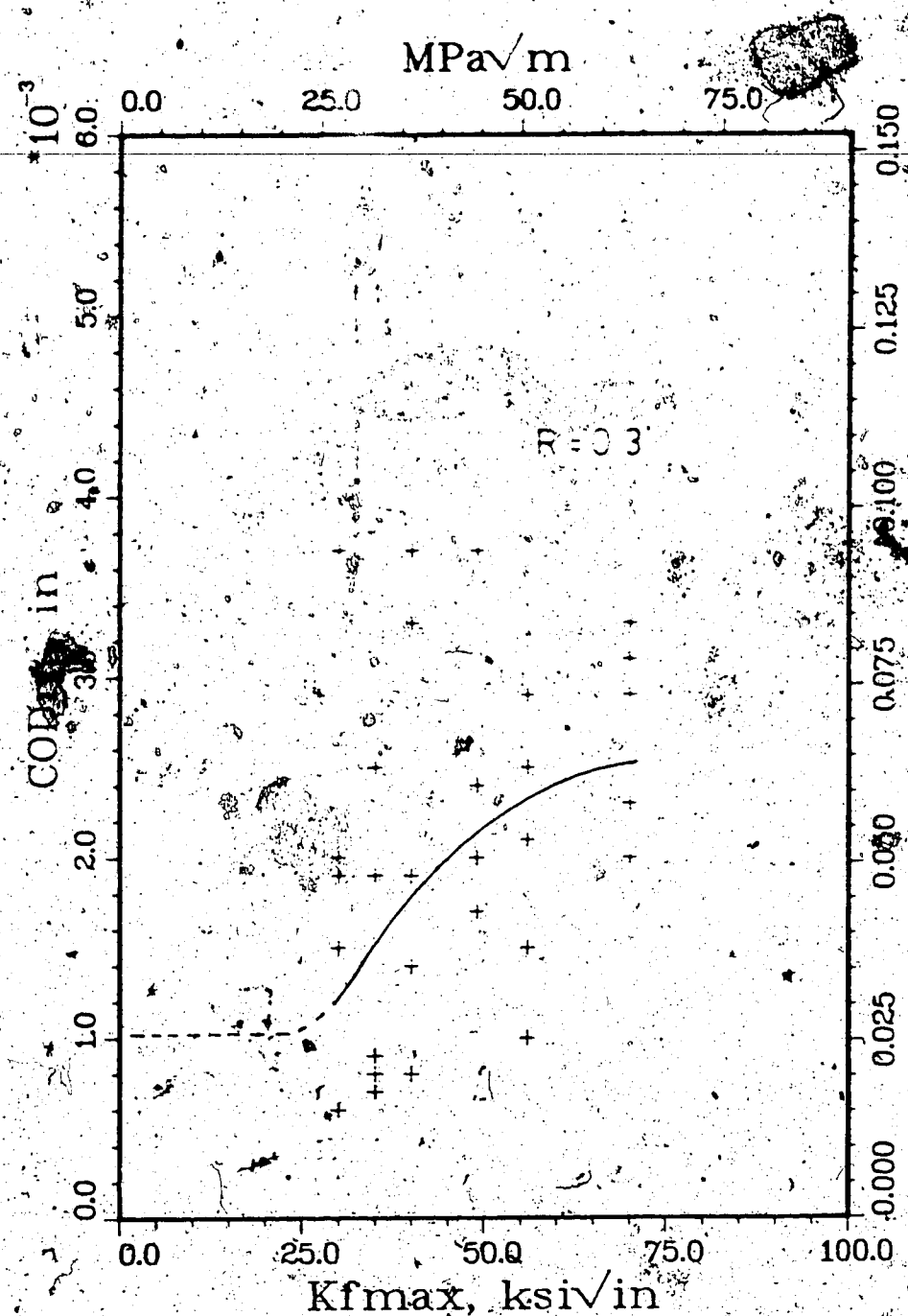
MPa√m
0.0
25.0
50.0
75.0
10^{-3}
6.0
5.0
4.0
3.0
2.0
1.0
0.0
COD, in
0.150
0.125
0.100
0.075
0.050
0.025
0.000
mm
R = 0.3
0.0
25.0
50.0
75.0
100.0
Kfmax, ksi√in

(b)

Figure 26

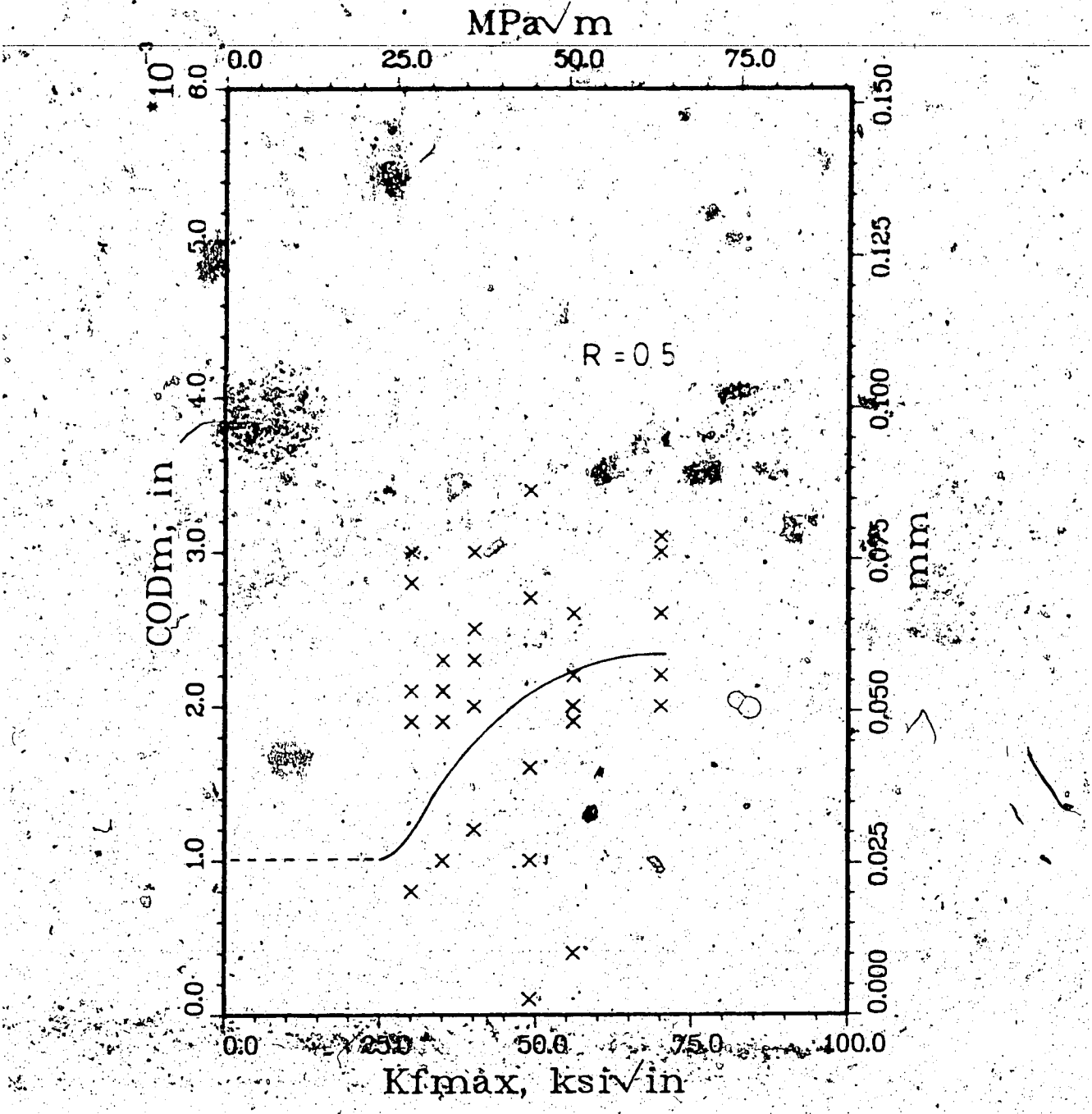
MPa√m
0.0
25.0
50.0
75.0
$\times 10^{-3}$
8.0
5.0
4.0
3.0
2.0
1.0
0.0
CODm, in
R = 0.5
0.150
0.125
0.100
0.075
0.050
0.025
0.000
mm
0.0
25.0
50.0
75.0
100.0
Kfmax, ksi√in

(c)

Figure 26

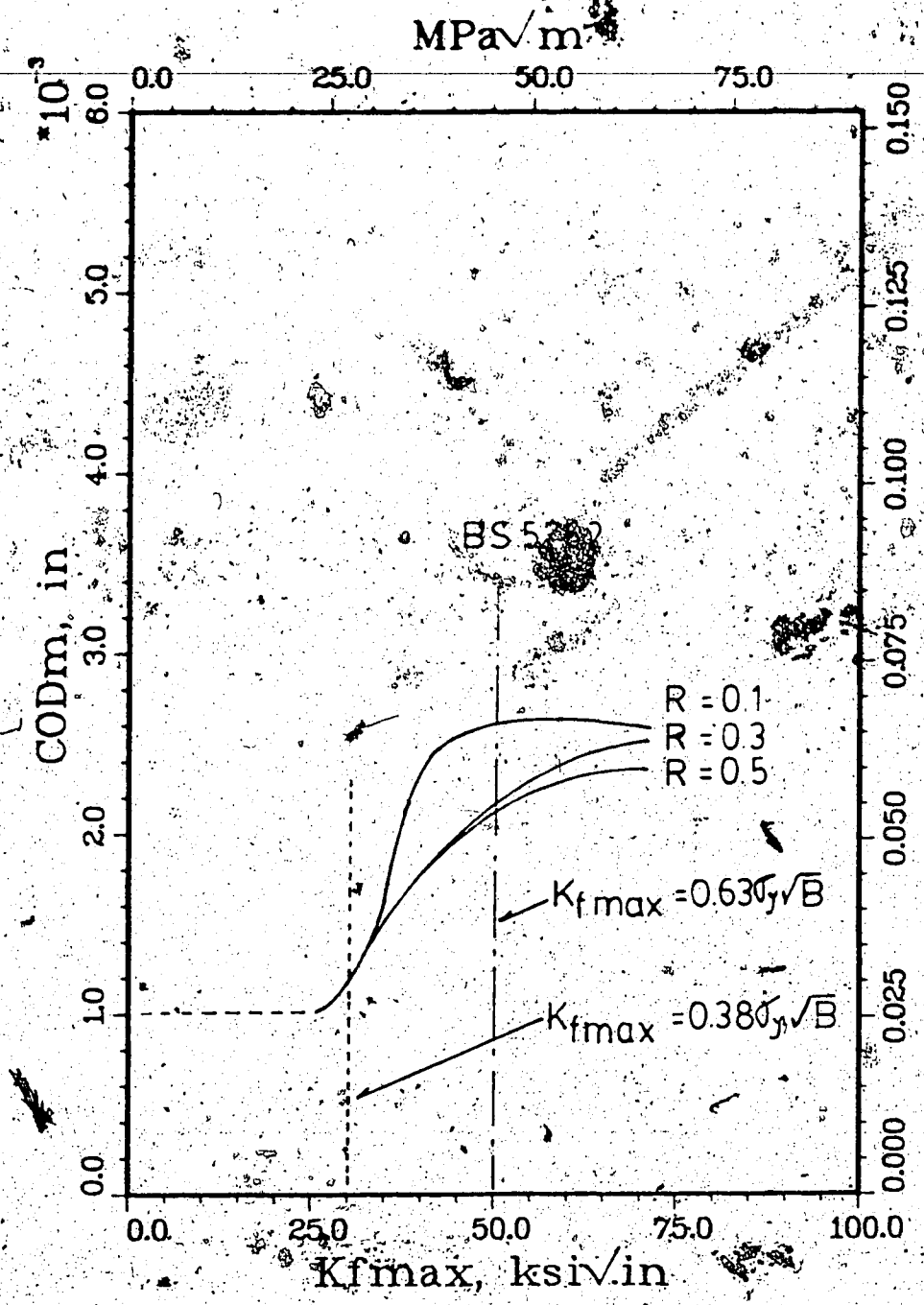
MPa√m
0.0
25.0
50.0
75.0
×10⁻³
8.0
5.0
4.0
3.0
2.0
1.0
0.0
CODm, in
0.150
0.125
0.100
0.075
0.050
0.025
0.000
mm
BS 5
R = 0.1
R = 0.3
R = 0.5
Kf max =0.63σy√B
Kfmax =0.38σy√B
0.0
25.0
50.0
75.0
100.0
Kfmax, ksi√in

(d)

Figure 26

Assuming that the lower limit value for Kq (Kql) is 70 ksi√in, the limiting Kfmax value is 0.6x70 = 42 ksi√in (38.2 MPa√m) for the ASTM E-399 and 0.7x70 = 49 ksi√in (44.5MPa√m) for the BS 5447. As shown in Fig.25(d), both restrictions on Kfmax did not quite ensure evaluation of a lower Kq value. Kfmax less than 0.42xKq might be a more appropriate limit for the material used in this experiment.

The limiting Kfmax value for the COD test is less than or equal to [redacted] or Kfmax ≤ 53 ksi√in (48.2 MPa√m). From Fig. [redacted] is evident that the Kfmax restriction given by th[redacted] standard failed to prevent over-estimation of the δm value. A more appropriate Kfmax value would be about 30 ksi√in or $0.38\sigma_y\sqrt{B}$. With this Kfmax value, the monotonic plastic zone size is approximately one eightieth of the specimen thickness; a factor of 0.6 smaller than the allowable plastic zone size given by the standard.

Table 4 Kq and CODm values obtained for different Kfmax and R-ratio

Kfmax	R = 0.1		R = 0.3		R = 0.5	
	Kq	CODm	Kq	CODm	Kq	CODm
(ksi√in)	(ksi√in)	10^{-3}in	(ksi√in)	10^{-3}in	(ksi√in)	10^{-3}in
30.00	70.20	1.2	73.80	2.0	72.90	2.8
30.00	69.30	1.1	73.90	1.5	74.10	3.0
30.00	7.50	1.5	72.60	1.9	76.60	2.1
30.00	71.30	0.7	78.00	3.7	68.98	8.0
30.00	72.20	0.8	63.50	0.6	74.34	1.9
35.00	73.40	1.7	73.30	2	76.60	2.3
35.00	72.60	1.2	74.30	1.9	73.90	2.1
35.00	74.50	2.0	67.97	0.7	77.00	2.1
35.00	73.00	1.8	70.80	0.9	73.20	1.0
35.00	71.00	1.6	70.10	0.8	74.65	1.9
40.00	75.30	2.1	74.50	1.4	72.50	1.2
40.00	72.70	3.1	61.60	3.3	74.60	2.3
40.00	74.40	3.0	67.70	0.8	71.40	2.0
40.00	75.30	2.5	67.90	1.9	75.00	2.5
40.00	75.60	3.0	74.90	3.7	70.00	3.0
49.00	72.80	2.7	74.40	2.0	72.50	0.1
49.00	82.90	2.4	75.20	3.7	69.20	3.4
49.00	81.10	3.1	78.20	1.7	72.50	1.6
49.00	77.00	2.6	78.20	2.0	66.60	1.0
49.00	78.20	2.0	77.00	2.4	73.30	2.7
56.00	78.70	3.3	71.66	1.0	73.50	2.6

56.00	80.40	1.6	78.75	2.9	79.30	1.9
56.00	78.00	2.9	71.10	2.1	60.00	0.4
56.00	82.90	2.3	74.10	1.5	75.90	2.2
56.00	78.75	2.9	74.70	2.5	75.90	2.0
70.00	75.30	1.6	74.60	3.1	75.50	3.0
70.00	75.30	3.0	75.90	2.9	76.60	2.2
70.00	78.90	2.2	76.20	2.0	77.80	3.1
70.00	79.30	2.8	74.60	2.3	75.30	2.6
70.00	77.40	2.5	77.40	3.3	74.30	2.0

7. Conclusions

Experiments with fatigue precracking fracture specimens for different values of Kfmax and R-ratio showed, as expected, that crack propagation rate increased with Kfmax. For a constant Kfmax value, the crack propagation rate increased as R decreased. This result indicates that the requirement by the K1c and COD standards for R≤0.1, maximizes the crack propagation rate.

The fracture test results for the specimens precracked at differing Kfmax indicated that both Kq and δm value increased with Kfmax until a limit was reached. The results indicated that, in order to evaluate a lower limit for Kq value, the Kfmax should be restricted to be less than 0.42Kq, considerably less than the standards allow. This demonstrates that for the material used in this investigation, the Kfmax restriction given by both K1c standards was not sufficiently stringent to avoid over-estimation of Kq value. Similarly, evaluation of lower δm values could only be obtained if the Kfmax value was less than $0.38\sigma_y/B$ which also indicated that the Kfmax restriction given by BS 5762 may be too high.

For a fixed Kfmax, limiting R≤0.1 results in a large stress intensity range and therefore a large reverse plastic zone. This type of crack tip is a poor approximation to the ideal plane crack. The fracture test result indicated that for a constant Kfmax, Kq increased as R decreased. Although a lower R value increased the crack propagation rate, the

use of higher values of R-ratio could be permitted and may even be necessary in order to minimize the reverse plastic zone size.

Results from this investigation illustrate that δm was affected by Kfmax, indicating that the production of a sharp fatigue crack is necessary and justifies the Kfmax restriction. Experiments regarding the effect of R-ratio on δm showed that there was greater scatter of δm when fatigue precracked at higher R. The overall results indicated insignificant difference in δm when R=0.1 as compared to R>0.1 was used.

Assuming that the mechanism responsible for the increased Kq and δm values is crack blunting due to the increase in both monotonic and reverse plastic zone size, the following conclusions can be made:

1. The monotonic plastic zone size should be minimized by minimizing the Kfmax value.
2. The reverse plastic zone size should be minimized by minimizing the ΔK value (ie. increased R-ratio when Kfmax is kept constant).
3. Lower values of R-ratio can be used when crack initiation is slow and need not be maintained low when the crack is propagating.

Acoustic emission monitoring during the fatigue precracking showed that the correlation of emission counts to propagating crack length was poor. Acoustic emission monitoring of the fatigue precracking of fracture specimens,

however, offered a good indication of the extent of plastic deformation due to monotonic or reverse loading at the crack tip.

Acoustic emission detection during the fracture test helped to indicate the initiation of the unstable crack growth. The total emission prior to fracture did not correlate well with the stress intensity factor value. This may have been due to differences in load ratios and maximum loads for different specimens during precracking.

Bibliography

Experiments in Fatigue Cracking and Fracture Toughness Test

ANSI/ASTM E-399:81,(1981),Standard Test Method for Plane Strain Fracture Toughness of Metallic Materials.

ASTM E-647:81,(1981),Standard Test Method for Constant Load Amplitude Fatigue Crack Growth Rates above 10 m/cycle.

ASTM E-561:81,(1981),Standard Practice for R-curve determination.

ASTM E-813:81,(1981),Standard Test for J1c A Measure of Fracture Toughness.

ASTM E-8:81,(1981),Standard Methods of Tension Testing of Metallic Materials.

Broek,D., *Elementary Engineering Fracture Mechanincs*, Noordhoff International Publishing, Leyden 1974.

British Standards Institution DD3:1971 ,Methods for Plane Strain Fracture Toughness (K1c) Testing.

British Standards Institution BS 5447:1977 , Methods of Test [illegible]lane Strain Fracture Toughness (K1c) of [illegible]ic Materials.

British [illegible]s Institution BS 5762:1979 , Methods for Crack Opening Displacement (COD) Testing.

Brown,W.F.Jr.,Srawley,J.E.,(1970),"Commentary on Present Practice," Review of Development in Plane Strain Fracture Toughness Testing, ASTM STP 463, 1970, pp216-248.

Burdekin.F.M.,Stone.D.E.W.,(1966),"The Crack Opening Displacement Approach to Fracture Mechanics in Yielding Materials", Journal of Strain Analysis Vol 1 No 2.

Clark,G.,(1979),"Significance of Fatigue Stress Intensity in Fracture Toughness Testing", International Journal of Fracture, 15, R179-R181.

Dowling,N.E.,(1977),"Fatigue Crack Growth Rate Testing at High Stress Intensities", ASTM STP 631, American

Society for Testing and Materials, pp139-58.

Dugdale.D.S.,(1960),"Yielding of Steel Containing Slits", Journal of the Mechanics and Physics of Solids, Vol 8, pp100-104.

Elber,W.,(1971),"The Significant of Fatigue Crack Closure," ASTM STP 486, pp230-242.

Irwin,G.R.,(1957),"Analysis of Stresses and Strains near the End of a Crack Traversing a Plate," Transactions, ASME, Journal of Applied Mechanics, Vol 24.

Jones,M.H.,Brown,W.F.,Jnr.(1977), Written discussion to 'Experience in plane-strain fracture toughness testing per ASTM method E-399' by J.G.Kaufman, STP 632, pp3-24.

Kaufman,J.G.,Schilling,P.E.,(1973),"Influence of Stress Intensity Level during Fatigue Cracking on Results of Plane-Strain Fracture Toughness Test", ASTM STP 536, pp312-319.

Kaufman,J.G.,(1977),"Experience in Plane Strain Fracture Toughness Testing per ASTM Method E 399," ASTM STP 632, pp3-24.

Klesnil,M.,Lukas,P.,*Fatigue of Metallic Materials*, Material Science Monographs, 7, Elsvier Scientific Publishing Company, Amsterdam 1980.

Knott,J.F.,*Fundamentals of Fracture Mechanics*, London, Butterworths 1973.

Kocanda,S.,*Fatigue Failure of Metals*, Sijthoff and Noordoff International Publishers 1978.

May,M.J.,(1970),"British Experience with Plane Strain Fracture Toughness (K1c) Testing", ASTM STP 463, American Society for Testing and Materials, pp41-82.

Maddox,S.J.,Gurney,T.R.,Mummery,A.M.,Booth,G.S.,(1978), "An investigation of the Influence of Applied Stress Ratio on Fatigue Crack Propagation in Structural Steels", Welding Institute Report 72/1978/E, September.

Paris,P.C.,Erdogan,F.,(1963),"A Critical Analysis of Crack Propagation Laws", Transactions of the ASME, Journal of Basic Engineering, Series D, 85, No 3, 1963.

Parker,A.P.,*The Mechanics of Fracture and Fatigue*, London,

E. and F.N. Spon Ltd. 1981.

Richards,C.E.,(1981),"Some Guidelines to the Selection of Techniques",The Measurement of Crack Length and Shape During Fracture and Fatigue, Beevers,C,J., Ed., Emas Enginering Materials Advisory Services Ltd., pp 461-68.

Rice.J.R.,(1968),"A Path Independent Integral and the Appoximate Analysis of Strain Concentration by Notches and Cracks", Journal of Applied Mechanics, Transaction ASME, 35, June.

Robinson,J.N.,Tetelman,A.S.,(1973),"Measurement of K1c on Small Specimen using Critical Crack Tip Opening Displacement" ASTM STP 559, American Society for Testing and Materials, pp 139-58.

Rolfe,S.T.,Barsom J.M., *Fracture and Fatigue Control in Structures. Application of Fracture Mechanics.* Prentice-Hall,Inc., Englewood Cliffs, New Jersey 1977.

Roman,I.,Ono,K.,Tetelman,A.S.,(1981), "The Effect of Cyclic Loading on the Apparent Cleavage Fracture Toughness of 1Cr-Mo-V Rotor Steel", Engineering Fracture Mechanics, 14, pp155-63.

Schmidt,R.A.,Paris,P.C.,(1973),"Threshold for Fatigue Crack Propagation and Effects of Load Ratio and Frequency", ASTM STP 536, American Society for Testing and Materials, pp79-94.

Smith.R.W.,Hirschberg,M.H.,Manson,S.S.,(1963), "Fatigue Behaviour of Materials under Strain Cycling in Low and Intermidiate Life Range", NASA Report TND-1574, April.

Towers,O.L.,(1981),"The Influence of Fatiquing Load and R-ratio on Fracture Toughness", The Welding Institute, June, 7709.02/81/257.3.

Yeh,T.,Burck,L.H.,(1979),"Cyclic Crack Opening Displacement behaviour during High-amplitude Block Loading", Engineering Fracture Mechanics, Vol.12, pp541-49.

Wells,A.A.,(1961), "Unstable Crack Propagation in Metals-Cleavage and Fast Fracture", Cranfield Crack Propagation Symposium, 1, Sept, p210.
Wells,A.A.,(1969),"Crack Opening Displacements from Elastic-Plastic Analysis of Externally Notched Tension Bars", Engineering Fracture Mechanics, Vol 1, pp399-410.

Westergaard,H.M.,(1939),"Bearing Pressure and Cracks", Transactions, ASME, Journal of Applied Mechanics, 61, ppA49-53.

Acoustic Emission general

Clark,G.,Knott,J.F.,(1977),"Acoustic Emission and Ductile Crack Growth in Pressure-vessel Steels", Metal Science, Nov, pp531-36.

Dunegan,H.L.,Harris,D.O.,Tatro,C.A.,(1968), "Fracture Analysis by use of Acoustic Emission", Engineering Fracture Mechanics, Vol 1, pp105-122.

Gerberich,W.W.,Hartbower,C.E.,(1967),"Some Observation on Stress Wave Emission as A Measure of Crack Growth", International Journal on Fracture Mechanics, Vol.3, Sept, pp185-91.

Harris,D.O.,Dunegan,H.L.,(1973),"Continuous Monitoring of Fatigue Crack Growth by Acoustic Emission Techniques, Dunegan/Endevco Technical Report DE-73-2.(February).

Harris,D.O.,Bell,R.L.,(1977),"The Measurement and Significance of Energy in Acoustic Emission Testing", Experimental Mechanics, Sep, pp347-53.

Lindley,T.C.,Palmer,I.G.,Richards,C.E.,(1978),"Acoustic Emission Monitoring of Fatigue Crack Growth", Material Science and Engineering, 32, pp1-15.

Lenain,J.C.,(1981),"General Principles of Acoustic Emission", Materials Evaluation, 39, Oct, pp1000-02.

Masounave,J.,Lanteigne,J.,Bassim,M.N.,Hay,D.R.,(1976), "Acoustic Emission and Fracture of Ductile Materials", Engineering Fracture Mechanics, Vol.8, pp701-09.

Mitsuru Arii, Hideo Kashiwaya, Tetsu Yanuki, (1975), "Slow Crack Growth and Acoustic Emission Characteristic in COD Test", Engineering Fracture Mechanics, Vol.7, pp551-56.

Morton,T,M.,Harrington,R.M.,Bjeletich,J.G.,(1973), "Acoustic Emission of Fatigue Crack Growth", Engineering Fracture Mechanics, Vol.5, pp691-97.

Palmer,I.G.,Heald,P.T.,(1973),"The Application of Acoustic Emission Measurements to Fracture Mechanics", Matrial Science and Engineering, 11, pp181-84.

Protasov,A.K.,Rybin,V.M.,(1979),"Increasing The Noise Immunity of Highly Sensitive Acoustic Emission Instruments", Industrial Laboratory, Vol.44, No.8, pp1132-34.

Radon,J.C.,Pollock,A.A.,(1972),"Acoustic Emissions and Energy Transfer during Crack Propagation", Engineering Fracture Mechanics, Vol.4, pp295-310.

Sinclair,A.C.E.,Formby,C.L.,Connors,D.C.,Darlaston,B.J.L., (1975),"Some Examples of Laboratory Application and Assesment of Acoustic Emission in The United Kingdom", Part II: Fatigue Crack Assesment from Proof Testing and Continuos Monitoring", ASTM STP 571, American Society for Testing and Materials, pp51-63.

The EWGAE Code for Acoustic Emission Examination- location of sources of discrete acoustic events, (1981), NDT International, August pp181-84.

Takahashi,H.,Khan,M.A.,Kikuchi,M.,Suzuki,M.,(1981), "Acoustic Emission Crack Monitoring in Fracture Toughness Test for AISI 4340 and SA533B steels", Experimental Mechanics, March, pp89-99.

APPENDIX 1 - Crack Propagation Measurement

Fatigue crack propagation measurements can be very tedious and time consuming (optical method), expensive (use of crack gauges) or complex (ultrasonic, electrical potential, compliance).

Compliance methods of crack measurement, however, can be simplified when used for fatigue precracking under constant mean load. The procedure is as follows; for the case of the three-point bend specimen, provided the applied load (P) is low (no generalised yielding at the specimen existed), there exists a relationship that relates the crack length and the clip gauge opening. A similar triangle can be established for two pairs of crack length vs clip gauge opening and expressed as

$$Vg'/Vg = \{a' + p(w-a')\}/\{a + p(w-a)\} \quad , \qquad (A1)$$

see Fig.I for definition of terms.

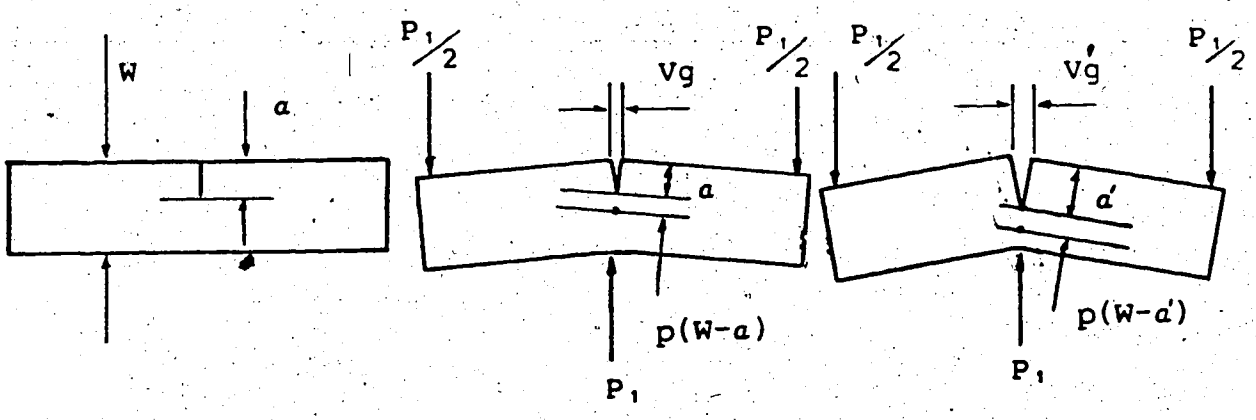

Figure I Relationship of crack length to clip-gauge displacement

Substituting $a' = a + \Delta a$

$Vg' = Vg + \beta \Delta Vg$

$p = 1/q$

Eq.A1 can be written as

$$\Delta a = \beta \Delta Vg \{w + (q-1)a\}/Vg(q-1) \quad (A2)$$

Based on the experimental value of Robinson and Tetelman (1973), the p value of 1/12 is used for small loads, this correspond to $(q-1)=11$. Therefore

$$\Delta a = \{\beta \Delta Vg / Vg\} \{(w+11a)/11\} \quad (A3)$$

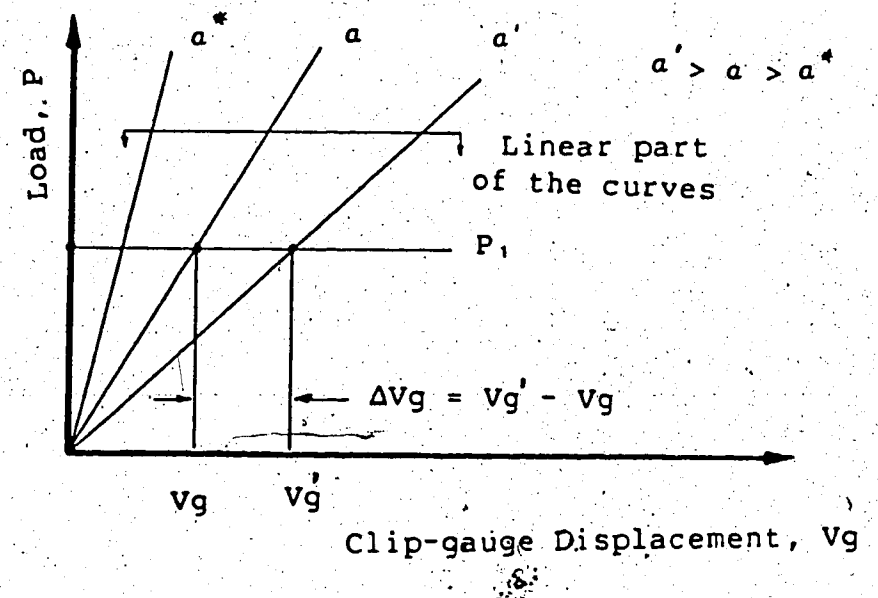

Figure II Load versus displacement curves for different crack length of three-point bend specimen

The value of β was evaluated using specimens of different notch depth, simulating different crack lengths. As shown in

Fig.II, the load versus clip gauge displacement of different crack length gives the necessary data to evaluate β. The experiment yielded β = 1/3.5 , hence, Eqn.A2 is expressed as

$$\Delta a = \Delta Vg\{w+11a\}/38.5Vg \qquad (A4)$$

The practical implications of this equation are simple. When fatigue precracking a fracture specimen, the initial crack length a and the width W are known. The clip gauge displacement Vg is measured as the relative displacement between a condition of no load and at the applied mean load (Pmean). Provided the mean load is kept constant (which is normally done with most load control fatigue machines), the value of ΔVg determines Δa. Measurement of ΔVg is done by subtracting the mean clip gauge displacements that correspond to crack length a' and a. The mean clip gauge displacement signal is obtained by low pass filtering the cyclic clip gauge signal.

Direct comparison of the above method with measurement by a crack gauge (see Fig.IV) is shown in Fig.III. Notice that disagreement occurs at the begining of the load cycle suggesting that the initiation has happened long before the crack gauge detected it. Later examination revealed that during the starting of the resonance type of fatigue machine, a stable mean load was not maintained.

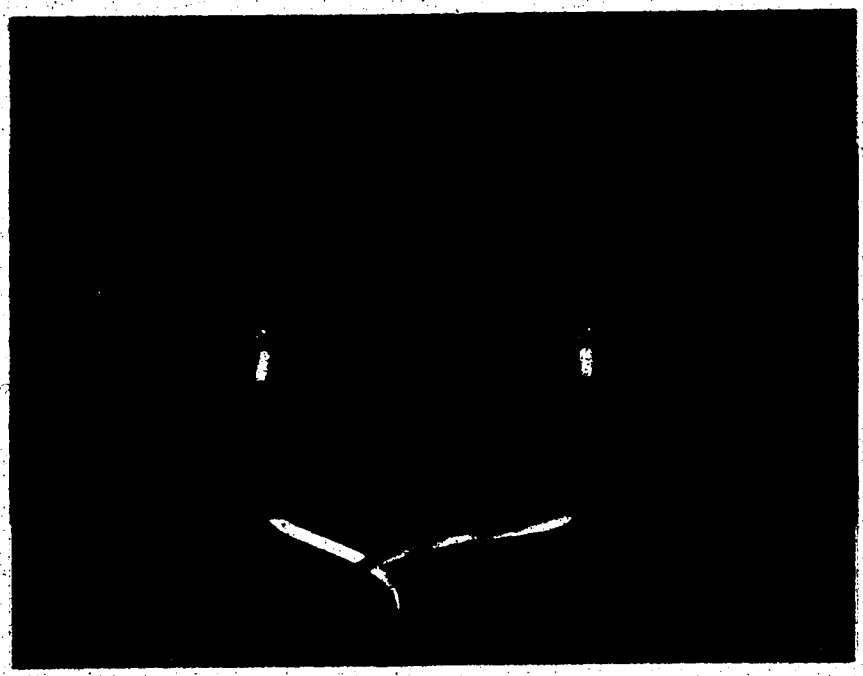

Figure III Measurement of crack length using crack-gauge TK-09-CPA01-005/S, Inter Technology Limited

Specimen A5

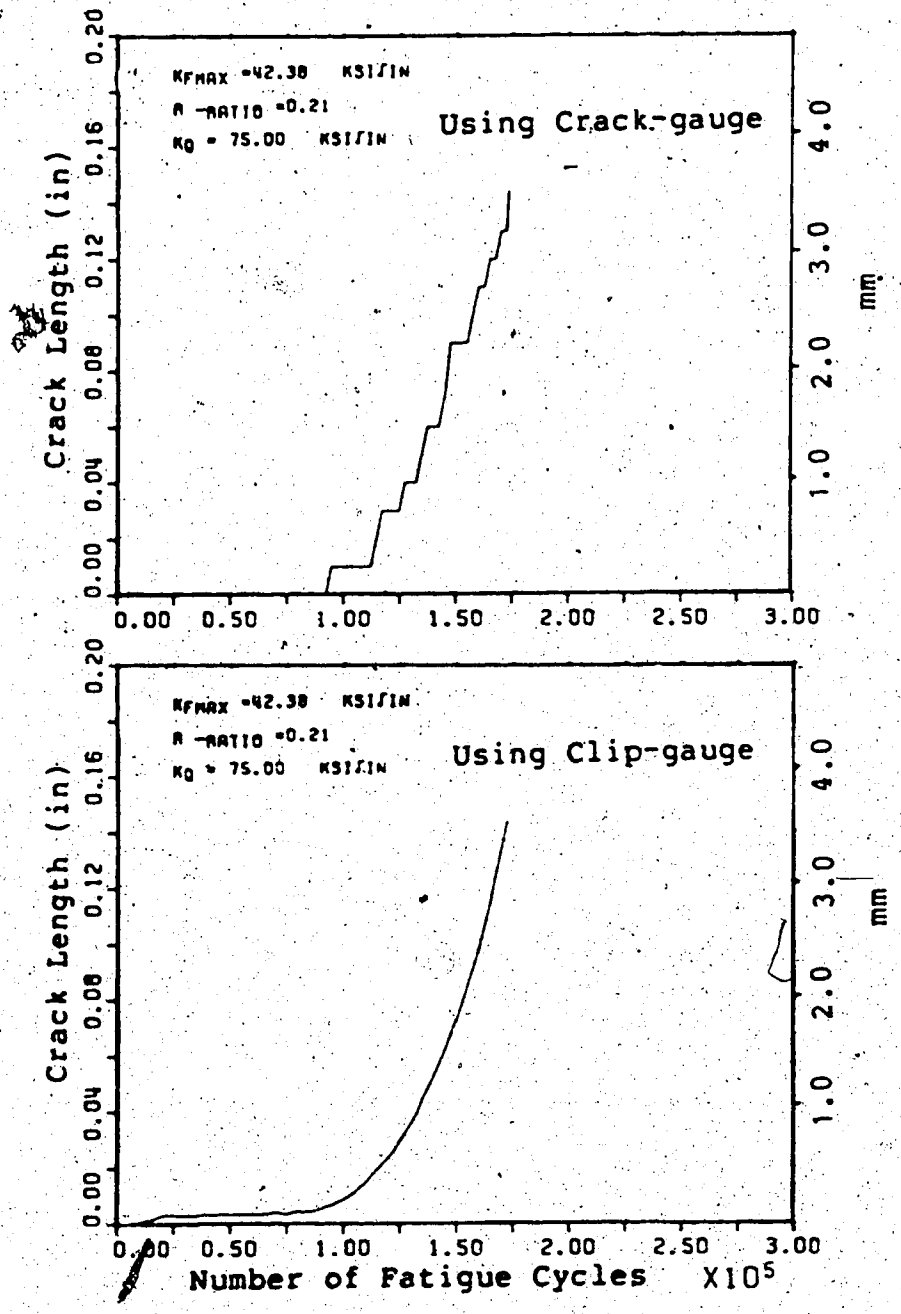

Figure IV Comparison of crack length measurement using (a)crack gauge and (b)clip-gauge

APPENDIX 2 - Preloading of Specimen for Acoustic Emission Test

Acoustic emission monitoring of a specimen requires an isolation or elimination of emission of noise from regions other than the test section. In some cases this noise could not be eliminated by specimen design and required additional techniques.

An elimination method that was used by Dunegan et al (1968) was preloading the unwanted region of the specimen. The preloading procedure was intended to use the Kaiser effect* which would result in no emissions from the preloaded region during the actual test loading. This preloading was done in a fixture shown in Fig.V.

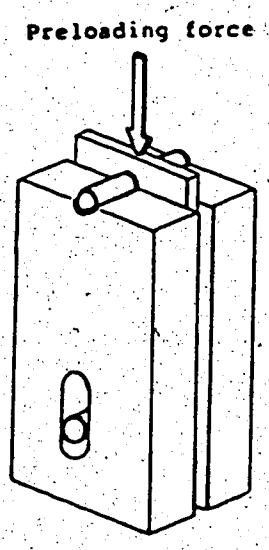

Figure V Preloading fixture (ref: Dunegan et al, 1968)

---

* The Kaiser effect is the absence of detectable acoustic emission at a fixed sensitivity level, until previously applied stress levels are exceeded (ref: ASTM E 610-82).

A photo-elastic study on the effectiveness of this preloading was done by Budney and Pettett (unpublished experiments) and is shown in Fig.VI. These photographs revealed that the stress pattern about the pin resulting from above preloading procedures did not resemble the stress pattern about the pin produced by the actual tension test. Thus such preloading did not effectively eliminate all the unwanted emission.

(a) (b) (c)

Figure VI Photo-elastic stress pattern of single-edge-notch fracture toughness specimen: (a)Preloaded as suggested by Dunegan et al, 1968. (b)Loaded in tension. (c)Overall view of the specimen loaded in tension

APPENDIX 3 - Data Acquisition

Experiments investigating the effects of maximum fatigue stress intensity factor (Kfmax) and stress ratio (R) on the fracture toughness value required the following data to be recorded:

a)Applied mean load.

b)Applied dynamic load.

c)Fatigue frequency.

d)Propagating crack length.

e)Number of cycles.

In this study acoustic emission ring down counts was also monitored throughout the period of fatigue precracking. During fatigue precracking acoustic emission ring down counts often overloaded the counter. Hence, it was necessary to reset the acoustic emission device at fixed intervals.

A data aquisition system was custom made for the above requirements resulting in a system illustrated in Fig.VII. The system included:

A)For the load signal

1)An amplifier for the load cell signal from a Vibrophore fatigue machine.

2)A frequency to voltage converter.

3)A peak detector which measured maximum applied load.

4)A lowpass filter which measured mean applied load.

5)A digital counter to count the number of fatigue

cycles.

6)A divider counter which produced a reset signal for any desired number of fatigue cycles.

B)For the clip gauge signal.

1)A clip gauge conditioner/amplifier (Vishay 2110/2120).

2)A lowpass filter to measure the mean clip gauge displacement.

3)A voltmeter.

C)For acoustic emission detection.

1)A Dunegan/Endevco 3000 system.

2)An oscilloscope.

D)For the control box.

1)A digital multiplexer.

2)An analogue to digital converter.

3)A central processing unit based on Motorola 6809.

E)For the recorder

1)Tektronix 4923 digital cartridge tape recorder.

The recorded data were transfered and processed with the University of Alberta MTS system (Michigan Terminal System) which uses an Amdahl 5960 computer.

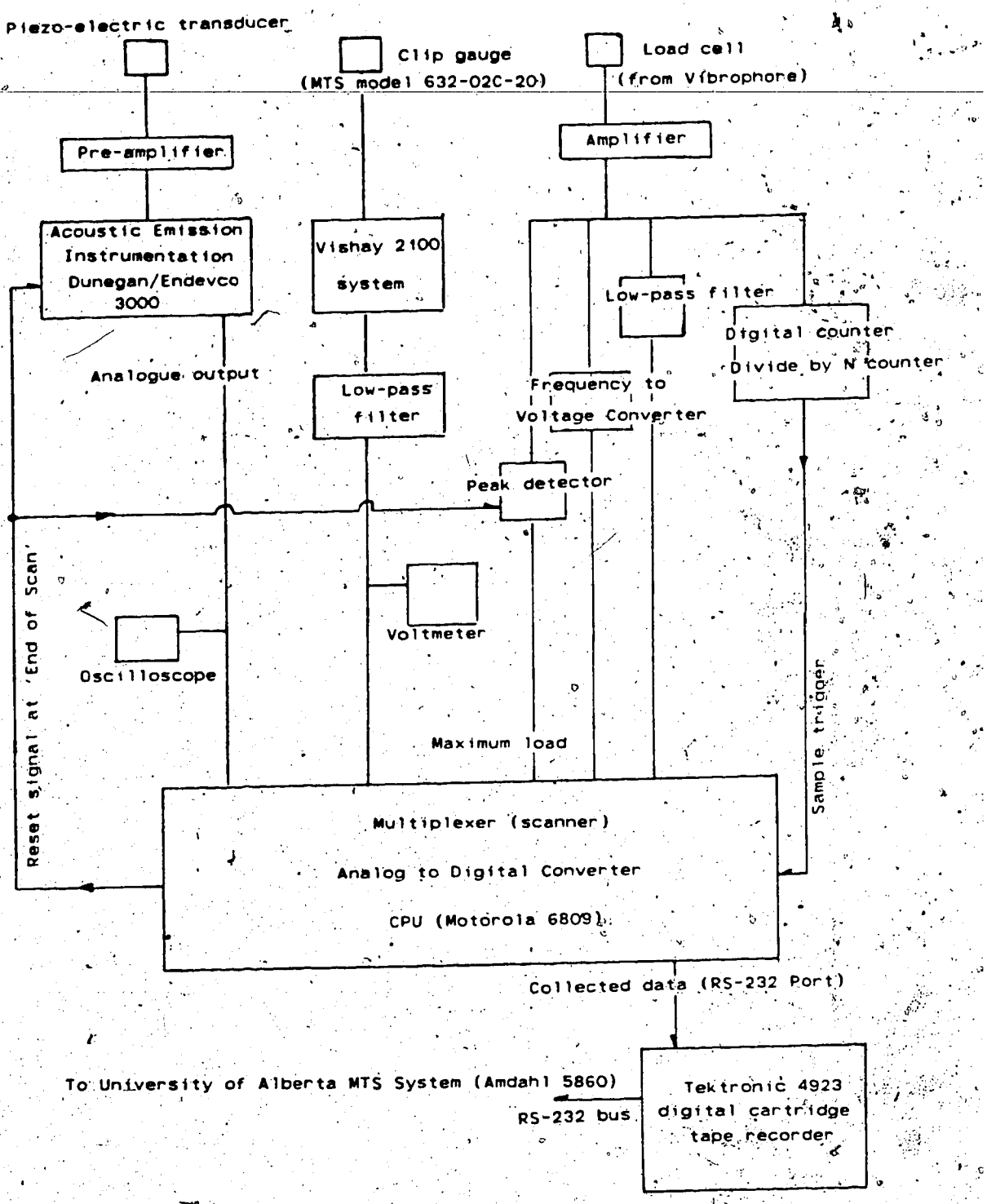

Figure VII Block diagram for data acquisition system for fatigue precracking of fracture specimens